Directional Curvature from Armijo Backtracking: A Low-Cost Sharpness Probe and a Calibration-Free Learning-Rate Safeguard for Adam

Anonymous authors
Paper under double-blind review

Abstract

The local sharpness of the loss, the top Hessian eigenvalue λ_1, determines the largest stable gradient step, but measuring it normally requires Lanczos or Hessian-vector iterations. We observe that a single Armijo backtracking line search already carries this information at the cost of a few forward passes: the accepted step α brackets the *directional* curvature $q = g^\top Hg/\|g\|^2$ within the multiplicative band set by the backtracking factor. Across CIFAR-10, Fashion-MNIST and Imagenette, $\log \alpha$ tracks $\log \lambda_1$ at Pearson -0.91 to -0.95, giving a low-cost online Edge-of-Stability reading. Used once at initialisation, this measurement yields a learning-rate cap (a safeguard, not a faster optimiser) that makes Adam robust to a too-large initial learning rate across more than three orders of magnitude (10^{-3} to 3.0), at about one percent overhead, and it is a no-op when the chosen rate is already safe. One probe is enough: periodic in-training probing adds no robust benefit. The raw-gradient probe exposes the mechanism but needs a safety factor calibrated to the architecture by a one-minute divergence sweep. Probing along Adam's own update direction removes this calibration: a single fixed safety factor $\kappa = 2$ avoids divergence on all nine architectures we test and across the full learning-rate grids of all four benchmarks, and the recipe transfers to AdamW unchanged.

1 Introduction

Adam (Kingma & Ba, 2015) and its variants (AdamW (Loshchilov & Hutter, 2019), NAdam (Dozat, 2016), AMSGrad (Reddi et al., 2018)) are the workhorses of contemporary deep learning. Their per-parameter adaptive scaling absorbs much of the heterogeneity of neural-network gradients and, in practice, decouples optimisation from the worst aspects of architecture-specific gradient geometry. What they do not absorb is the user's choice of *initial* learning rate. An η chosen one order of magnitude too large drives the loss to numerical infinity within a handful of steps, well before Adam's running estimates of the second moment have accumulated enough mass to dampen the update. The result is a single divergent first step, after which the entire training run is wasted.

The community has developed several pragmatic responses to this problem. The most principled is the explicit learning-rate range test (Smith, 2017; Smith & Topin, 2019), which trains a model for one or more epochs while sweeping the learning rate and inspects the loss–learning-rate curve for the largest still-stable value. A second line of work removes the learning rate from the user interface entirely by inferring it from running estimates of online-convex-optimisation quantities; D-Adaptation (Defazio & Mishchenko, 2023), Prodigy (Mishchenko & Defazio, 2024), Mechanic (Cutkosky et al., 2023) and the Schedule-Free family (Defazio et al., 2024) are the most recent and most visible representatives. A third, far less elegant but in practice ubiquitous approach is for users to manually iterate over a few candidate values and to discard whatever diverges. None of the three provides a low-cost, calibrate-once safety check that a particular chosen η is safe.

We propose a fourth route, designed to coexist with rather than replace any of the above. Before the first Adam update, we run a single Armijo backtracking line search (Armijo, 1966) at the randomly initialised parameters:

starting from $\alpha = 1$, we backtrack along the negative initial gradient until the standard sufficient-decrease condition is satisfied. The resulting step size $\bar{\alpha}_{\text{init}}$ is a one-batch empirical estimate of the largest stable gradient step at initialisation. If the user's η_{init} exceeds $\kappa \cdot \bar{\alpha}_{\text{init}}$ for a small safety constant κ, the optimiser silently lowers η_{init} to $\kappa \cdot \bar{\alpha}_{\text{init}}$ before its first update; otherwise it leaves the user's choice untouched. The probe costs approximately one fresh forward-and-backward pass plus a handful of forward-only backtracking evaluations, totalling under fifty milliseconds on a single RTX 6000. The rescue is intentionally minimal: vanilla Adam runs unchanged afterwards. The probe comes in two variants with distinct roles in this paper. The *raw-gradient* probe admits a clean link to the Hessian spectrum and is our measuring instrument throughout; the *direction-matched* probe, which searches along Adam's own update direction, needs no per-architecture calibration and is the variant we recommend as the default safeguard, with a single fixed safety factor $\kappa = 2$ across every architecture we test (Table 9).

The central claim of this paper is therefore first a *measurement* claim, and only then a practical one. On a convex quadratic loss, exact line search along the negative gradient gives $\alpha^\star = 1/q$, where $q = g^\top Hg/\|g\|^2 \leq \lambda_1$ is the directional curvature; equivalently $1/\alpha^\star$ reads curvature along the gradient and is upper-bounded by λ_1. We show this textbook relation survives into deep networks in a precise, usable form (Section 3, 5): the Armijo step inverts the *directional* curvature $q = g^\top Hg/\|g\|^2$ up to the multiplicative backtracking band, and q in turn tracks λ_1, so across CIFAR-10/ResNet-18, Fashion-MNIST/CNN and Imagenette/ResNet-18 (three seeds each, over 2000 step–probe pairs) $\log \alpha$ and $\log \lambda_1$ correlate at Pearson -0.91 to -0.95. The line search is thus a low-cost online sharpness sensor (~ 5 forward passes, no Hessian-vector products), giving an Edge-of-Stability reading (Cohen et al., 2021; Lewkowycz et al., 2020; Damian et al., 2023; Andreyev & Beneventano, 2024) that the literature normally obtains with Lanczos iteration.

We then ask what this measurement buys in practice. Used once at initialisation, the probe caps a too-large learning rate: on CIFAR-10/ResNet-18 vanilla Adam diverges in the first step for any $\eta \geq 0.1$, whereas the init-probe variant holds test accuracy in $[0.79, 0.83]$ across $\eta \in [10^{-3}, 3.0]$ (5 seeds) at about one percent overhead. Two more elaborate periodic controllers (*watchdog*, *tracker*) match the one-shot probe on CIFAR-10 but do not transfer to other settings and add no robust benefit; we therefore recommend the one-shot probe.

In summary, this paper contributes: *(i)* the observation, with an exact bracketing of q and a strong empirical α–λ_1 correlation across three architectures, that the Armijo line-search step is a low-cost, Hessian-free online estimate of local curvature, in effect an Edge-of-Stability reading for the price of a few forward passes (Section 5); *(ii)* a one-shot *init probe* built on this measurement that caps Adam's initial learning rate, a low-overhead, calibrate-once-then-deploy safeguard against learning-rate misspecification (Section 3); and *(iii)* a controlled delineation of where learning-rate control helps and where it does not, across CIFAR-10, Fashion-MNIST, Imagenette and AG News, and against gradient clipping (Pascanu et al., 2013) and warmup (Goyal et al., 2017).

We make two claims. The first is a measurement claim: the Armijo step reads local curvature. Wherever the backtracking constraint binds, $1/\alpha$ brackets the directional curvature q within the factor-$1/\beta$ band, and it tracks the top eigenvalue λ_1 both as a static correlation (Table 1) and online over training (Figure 2), at the fidelity characterised in Table 2; this α–λ_1 link is a within-run effect on the tested architectures, not a universal law. The second is a rescue claim: used as a one-shot cap, the measurement makes Adam robust to a too-large initial learning rate where that rate is genuinely unsafe (Tables 3 and 8), and it is a no-op otherwise. Both claims concern safety rather than speed; periodic in-training probing, in particular, adds no robust benefit and can hurt (Table 11).

2 Related work

The oldest pragmatic response to learning-rate sensitivity is the range test. Smith (2017); Smith & Topin (2019) introduced an explicit range test in which a model is trained for a few epochs while the learning rate is exponentially increased; the inflection point of the loss curve indicates the largest safe learning rate. Range tests are robust and widely adopted, but they require one or more epochs of training as upfront cost. Our probe is structurally similar in spirit but strictly lighter: a single backtracking line search at initialisation, consisting of one forward–backward pass to obtain the direction plus on average five forward-only loss evaluations for backtracking.

A more radical recent line of work removes the learning rate from the interface altogether, proposing optimisers that automatically infer their own learning rate from running estimates of online-convex-optimisation quantities. D-Adaptation (Defazio & Mishchenko, 2023) maintains a running lower bound on the distance to a minimiser and uses it as the learning rate; the method is hyperparameter-free and provably matches the optimal convergence rate for convex Lipschitz problems. Prodigy (Mishchenko & Defazio, 2024) extends D-Adaptation by improving its convergence rate by a $\sqrt{\log(D/d_0)}$ factor. Mechanic (Cutkosky et al., 2023) tunes the scale factor of *any* base optimiser online, again grounded in online-convex-optimisation reductions. The Schedule-Free family (Defazio et al., 2024) removes both the learning-rate *schedule* and the requirement to specify the stopping time. All four methods modify the optimiser's internal state continuously; in contrast our probe sits next to Adam, runs once at initialisation (optionally every K_{probe} steps), and only adjusts a single scalar (Adam's η).

A third family assumes the base rate is already known and only shapes it over time. Cyclical learning rates (Smith, 2017), SGDR (Loshchilov & Hutter, 2017) and super-convergence (Smith & Topin, 2019) prescribe schedules on top of a known base learning rate. Linear warmup (Goyal et al., 2017) is the simplest example and is the closest baseline to our init probe; it is reactive (gradients can still explode if the warmup target is too high) rather than calibrated.

Closest to our mechanism is the stochastic line-search literature. Vaswani et al. (2019) (SLS) apply Armijo backtracking on each mini-batch. SLS uses the line search for the actual update, while we use it only as a probe and let Adam do the actual optimisation. The Polyak step of Loizou et al. (2021) and the parabolic approximation (Mutschler & Zell, 2020) are alternative non-standard adaptive step rules.

The reason a line-search probe carries so much information about the stable range is best understood through the Edge-of-Stability literature. Cohen et al. (2021) showed that *full-batch* gradient descent on a deep network at fixed η enters a regime where the top Hessian eigenvalue λ_1 rises until $\lambda_1 \approx 2/\eta$ and then oscillates around that value. The catapult mechanism (Lewkowycz et al., 2020), the theoretical analysis of Arora et al. (2022), and the implicit-bias study of Damian et al. (2023) are part of the same line. Most relevant to us is the recent extension to mini-batch SGD by Andreyev & Beneventano (2024), who show that what stabilises at $2/\eta$ in stochastic optimisation is not λ_1 but *Batch Sharpness*, the expected directional curvature of the mini-batch Hessian along the corresponding stochastic gradient. Our probe-batch line search measures essentially this directional curvature, which is why the empirical correlation we observe (Pearson -0.91 to -0.95 on log scale) is so tight in the mini-batch regime. The empirical methodology of all of these works relies on PyHessian-style (Yao et al., 2020) Lanczos / power iteration for explicit eigenvalue estimation, which is computationally expensive.

A closely related recent line reads curvature from forward passes rather than from Hessian-eigenvalue iterations. Kalra & Barkeshli (2024) choose η_{init} via the loss catapult mechanism, addressing the same too-large-initial-rate failure as our safeguard but by a different mechanism, and Kalra et al. (2026) design a two-phase line search along the update direction to estimate a *critical sharpness* $\lambda_c = 2/\eta_c$, which they use as a training-time diagnostic that tracks progressive sharpening and the Edge of Stability at LLM scale. Our finding is complementary. Rather than a purpose-built measure, the curvature signal is already carried by a standard Armijo sufficient-decrease backtracking search: the accepted step brackets the directional curvature within the multiplicative band of the backtracking factor, so a practitioner already running such a line search obtains the reading at no extra cost. We further turn a single reading at initialisation into a calibration-free learning-rate safeguard ($\kappa = 2$) rather than a diagnostic.

Building on this curvature view, the closest related work is Roulet et al. (2024), who analyse classical line-search and quadratic-fit tuners (PAL, Armijo backtracking) under the lens of curvature dynamics. They find empirically that classical tuners "undershoot the edge of stability", producing a snowball effect of ever-increasing sharpness and ever-decreasing learning rates; this matches what we observe for GS+Armijo on CIFAR-10/ResNet-18 (Appendix A). They propose CDAT, a continuous tuner that dynamically drives η toward the EoS. Our work is complementary: we focus on the mini-batch regime, treat the line search as a probe rather than as a tuner, and design our controllers (Watchdog, Tracker) to sit deliberately *below* the EoS at $\kappa\,\bar{\alpha} \approx \bar{\alpha}/4$, which trades a small amount of optimisation efficiency for divergence safety. Our practical contribution, the init-probe rescue, is to our knowledge not present in their work.

Finally, the simplest and most widely deployed defence is gradient clipping: Pascanu et al. (2013) introduced global gradient-norm clipping to combat exploding gradients in RNN training. Clipping bounds the update norm but not the implicit step into a sharp region, and we compare against it directly in our experiments.

3 Method

Throughout this section we denote the model parameters by θ, the loss on a mini-batch $\mathcal{B}$ by $L(\theta; \mathcal{B})$, and Adam's scalar learning rate by η. We assume the standard Adam update $\theta_{t+1} = \theta_t - \eta\, m_t/(\sqrt{v_t} + \varepsilon)$ with the default first- and second-moment estimates (Kingma & Ba, 2015); our controller never modifies these internal estimates and only adjusts the scalar η.

The core of our method is a single Armijo backtracking line search (Armijo, 1966) executed once, immediately before the first Adam update. Concretely, we sample the first training mini-batch $\mathcal{B}_0$, compute the loss $L_0 = L(\theta_0; \mathcal{B}_0)$ and gradient $g_0 = \nabla_\theta L(\theta_0; \mathcal{B}_0)$ at the random initialisation θ_0, and search for the largest step $\alpha \in (0, 1]$ along the descent direction $d_0 = -g_0$ that satisfies the standard sufficient-decrease (Armijo) condition $L(\theta_0 + \alpha d_0; \mathcal{B}_0) \leq L_0 - c\,\alpha\,\|g_0\|^2$. We initialise $\alpha = 1$ and shrink by a factor $\beta = \frac{1}{2}$ until the condition holds, capping the iteration at $K = 8$ backtracks. The resulting $\bar{\alpha}_{\text{init}}$ is a single-batch empirical estimate of the largest stable gradient step at initialisation. Algorithm 1 states the procedure compactly.

Algorithm 1 Init probe with safety cap (general descent direction d).

Input: model θ_0, loss L, mini-batch $\mathcal{B}_0$, direction rule d, safety factor κ, Armijo constants c, β, maximum backtracks K.
Variants: raw-gradient $d_0 = -g_0$ (mechanism, $\kappa = 0.25$); **direction-matched (recommended)** $d_0 = -g_0/(|g_0| + \varepsilon)$ (Adam's first-step geometry, $\kappa = 2$).
$L_0 \leftarrow L(\theta_0; \mathcal{B}_0)$, $g_0 \leftarrow \nabla L(\theta_0; \mathcal{B}_0)$
$\alpha \leftarrow 1$
for $k = 1, \ldots, K$ **do**
  if $L(\theta_0 + \alpha d_0; \mathcal{B}_0) \leq L_0 + c\,\alpha\, g_0^\top d_0$ **then**
    break ▷ Armijo holds: accept the tested α
  else if $k < K$ **then**
    $\alpha \leftarrow \beta\alpha$ ▷ shrink and retry
  else
    keep last tested α ▷ saturated after K backtracks; cap conservatively
  end if
end for
$\bar{\alpha}_{\text{init}} \leftarrow \alpha$
if $\eta_{\text{user}} > \kappa\,\bar{\alpha}_{\text{init}}$ **then** $\eta \leftarrow \kappa\,\bar{\alpha}_{\text{init}}$ **else** $\eta \leftarrow \eta_{\text{user}}$
Restore θ_0; start Adam at η.

The default value of the safety constant on CIFAR-10/ResNet-18 is $\kappa = 0.25$. We arrived at this number directly from the empirical divergence boundary of vanilla Adam reported in Appendix C: vanilla Adam first diverges at $\eta \approx 0.6\,\bar{\alpha}_{\text{init}}$, so a safety factor of $\kappa = 0.25$ leaves a comfortable margin of roughly $2\times$ without being overly conservative. The choice is forgiving: a sweep over κ (Appendix B) shows that any $\kappa \leq 0.25$ keeps the rescue intact on CIFAR-10, with graceful rather than catastrophic degradation beyond. *For the raw-gradient probe*, as Section 5 will show, κ is architecture-specific and a ∼one-minute divergence sweep is the recommended way to set it on a new architecture (once chosen it can be reused across hyperparameter searches and seeds); the direction-matched variant introduced next removes this dependence and uses a single fixed $\kappa = 2$ throughout.

Direction-matched Adam probe. The probe so far line-searches along $d_0 = -g_0$, but Adam does not step along the raw gradient. Its first update direction is $-m_0/(\sqrt{v_0} + \varepsilon)$; with bias correction at $t = 1$ this is $\hat{m}_0 = g_0$ and $\hat{v}_0 = g_0^2$, so Adam's first step points along

$$d_{\text{Adam}} \;=\; -\frac{g_0}{\sqrt{g_0^2} + \varepsilon} \;=\; -\frac{g_0}{|g_0| + \varepsilon} \;\approx\; -\operatorname{sign}(g_0),$$

the preconditioned direction in which the optimiser actually moves. The direction-matched variant of the probe runs the *same* backtracking search along d_{Adam} instead of $-g_0$, accepting the largest $\alpha \in (0, 1]$ that satisfies the general Armijo condition $L(\theta_0 + \alpha\, d_{\text{Adam}}; \mathcal{B}_0) \leq L_0 + c\, \alpha\, g_0^\top d_{\text{Adam}}$ (note $g_0^\top d_{\text{Adam}} < 0$), and caps the learning rate at $\eta \leq \kappa\, \bar{\alpha}_{\text{Adam}}$ exactly as in Algorithm 1. Because $\bar{\alpha}_{\text{Adam}}$ is now measured in Adam's own geometry, the conversion factor κ no longer has to absorb the per-architecture gradient scale: a single fixed value transfers across architectures, which we establish empirically in Section 5 (Table 9). This is the variant we recommend when a per-architecture divergence sweep is undesirable; the raw-gradient probe is retained in the body experiments because it admits the clean link to λ_1 used to expose the mechanism.

The init probe handles the most common failure mode, a single catastrophically wrong initial learning rate, but cannot react to sharpness changes during training. For users who want continuous in-training adaptation, we provide two periodic controllers that re-run the same Armijo probe every K_{probe} Adam steps (default $K_{\text{probe}} = 50$) and adjust η from the resulting α_t. The defensive *Watchdog* maintains a baseline $\bar{\alpha}_{\text{base}}$ from the first probe and shrinks η by a factor of two whenever $\alpha_t/\bar{\alpha}_{\text{base}}$ falls below 0.5; symmetrically it grows η by a factor of 1.2 when the ratio recovers above 0.8, but never beyond the user's initial value or below $0.05\,\eta_{\text{init}}$. The active *Tracker* simply chases the probed step via an exponential moving average, $\eta_{t+1} = (1 - \beta)\eta_t + \beta\kappa\alpha_t$, with the same κ as the init probe and $\beta = 0.1$. Both controllers were tuned by inspection on CIFAR-10/ResNet-18; we will see in Section 5 that their tuned thresholds do not transfer to a small CNN, and that on Fashion-MNIST it is in fact best to disable them and rely on the init probe alone.

As for compute, an init probe consumes one extra forward-and-backward pass at θ_0 (to obtain the descent direction) plus on average five *forward-only* backtracking evaluations, in total ~ 50 ms on a single RTX 6000. Because Adam-InitOnly fires this probe only once, its wall-clock overhead is about 1% on CIFAR-10/ResNet-18, within measurement noise of vanilla Adam. A periodic probe is structurally identical; with the default $K_{\text{probe}} = 50$ the periodic-probe controllers add a measured $\approx$2.7% (Adam-Tracker) to $\approx$5.3% (Adam-Watchdog) of wall-clock (Section 5). Evaluating the backtracking trials forward-only, rather than recomputing a gradient at every trial, roughly halves this periodic overhead.

4 Experimental setup

Our primary testbed is ResNet-18 with the standard CIFAR adaptation (3×3 stride-1 conv stem, no max-pool, no pre-trained weights), trained on CIFAR-10 (50k train / 10k test) with standard augmentation (random crop with 4-pixel padding, horizontal flip), batch size 256, for 10 epochs. On this testbed we benchmark five optimisers, all built on top of the same vanilla Adam implementation (`torch.optim.Adam` with $\beta_1 = 0.9$, $\beta_2 = 0.999$, $\varepsilon = 10^{-8}$). Three are our own contributions of varying complexity: *Adam-InitOnly*, which performs only the init probe of Section 3 and then leaves Adam alone; *Adam-Watchdog*, which additionally re-probes every fifty Adam steps and applies the defensive shrink/grow rule; and *Adam-Tracker*, which uses the same periodic probe but feeds it into the active EMA controller. Two are simple and widely deployed baselines that target similar failure modes: *Adam + grad-clip*, which clips the global gradient norm to one before each Adam update, and *Adam + linear warmup*, which initialises Adam at $\eta_{\text{init}}/100$ and ramps the learning rate linearly to η_{init} over the first 200 steps. Two recent parameter-free optimisers, Schedule-Free AdamW (Defazio et al., 2024) and Prodigy (Mishchenko & Defazio, 2024), complete the comparison in the rescue experiments. Adam-InitOnly uses the raw-gradient probe with a per-architecture κ unless marked "dir.", which denotes the direction-matched probe of Algorithm 1 at the fixed $\kappa = 2$.

Transfer beyond this primary setting is tested on three further benchmarks. Fashion-MNIST (60k train / 10k test) is trained with a small CNN (two convolutional and two fully-connected layers, 0.4M parameters); AG News topic classification (4 classes, 120k/7.6k train/test) with a small from-scratch encoder-only Transformer (4 layers, $d_{\text{model}} = 128$, word-level tokeniser); and Imagenette (Howard, 2019), the fastai ImageNet subset (10 classes, 9.5k/3.9k train/val images), trained at 128×128 with the standard full-stem ResNet-18 as a real-resolution control (Appendix F). Probe and controllers are identical across all four testbeds; only the data loader and model differ. The Fashion-MNIST CNN also serves as the second architecture in the mechanism experiments below, and the cross-architecture study of the direction-matched probe widens the set to nine models (normalisation variants, an MLP, an LSTM, and Transformers of several scales), introduced where they appear.

Each (optimiser, initial learning rate) combination is run with 5 seeds; we report mean ± standard deviation and divergence rate. In the optimiser-comparison tables, bold marks the best mean per column within each block of rows, since the blocks compare different regimes (standard baselines, probe controllers, parameter-free optimisers; uncalibrated versus calibrated); divergent, partially divergent and chance-level entries are not marked. A run is marked *diverged* if loss exceeds 5× initial or becomes `NaN`. The mini-batch loss is logged *before* each update, so the blow-up caused by the destabilising first update is recorded at the next logged step; throughout, "diverges in the first step" refers to this first update, which our logs flag within the first two logged steps. Hardware: single NVIDIA RTX 6000 Ada Generation per run. The experimental protocol (seeds, averaging, and how the overhead and curvature numbers were obtained) is detailed in Appendix G.

5 Results

We open with the measurement at the heart of the method: what the line-search step reveals about the local loss landscape, and at what cost. The init probe and the periodic probes both estimate, at very low cost, the largest gradient step that the local loss landscape can absorb. We make this connection precise, and we do it for a general descent direction d (with $g^\top d < 0$), because the direction along which the *optimiser* steps will matter below. On a quadratic loss $L(\theta) = \frac{1}{2}(\theta - \theta^\star)^\top H(\theta - \theta^\star)$ with $H \succ 0$, exact line search along d chooses the minimiser

$$\alpha^\star \;=\; \frac{-\,g^\top d}{d^\top H d} \;=\; \frac{1}{q_d}, \qquad q_d \;:=\; \frac{d^\top H d}{-\,g^\top d},$$

where q_d is the curvature *along* d. For the raw gradient $d = -g$ this is $q_{-g} = g^\top H g / \|g\|^2 \in [\lambda_n, \lambda_1]$, so $1/\lambda_1 \le \alpha^\star \le 1/\lambda_n$. Empirically we measure α and the top Hessian eigenvalue λ_1 throughout training of ResNet-18 on CIFAR-10 and, as cross-architecture checks, of a plain CNN on Fashion-MNIST and of the standard full-stem ResNet-18 on Imagenette at 128px. The results are reported in Table 1.

Table 1: Empirical correlation between the line-search step α and the top Hessian eigenvalue λ_1 along training, on CIFAR-10/ResNet-18, Fashion-MNIST/CNN and Imagenette with the standard full-stem ResNet-18 (10 epochs, $K_{\text{probe}} = 100$; Imagenette: 20 epochs, $K_{\text{probe}} = 30$, since its epochs are only 37 steps). Means over 3 seeds where indicated; p-value for the log–log Pearson.

Variant	$\bar{r}_{\log\alpha,\log\lambda_1}$	$\bar{r}_{\text{Spearman}}$	$\bar{p}$	$\bar{\alpha}$
Pure Armijo, CIFAR-10/ResNet-18 (3 seeds)	-0.913 ± 0.013	-0.83 ± 0.04	$< 10^{-7}$	0.666
Pure Armijo, Fashion-MNIST/CNN (3 seeds)	-0.950 ± 0.017	-0.89 ± 0.04	$< 10^{-10}$	0.292
Pure Armijo, Imagenette/ResNet-18 (3 seeds)	-0.907 ± 0.021	-0.85 ± 0.03	$< 10^{-8}$	0.274
Pure Armijo, Digits/MLP (1 seed)	-0.775	-0.61	0.024	0.95
GS+Armijo, CIFAR-10/ResNet-18 (1 seed, Appendix)	-0.32	-0.17	0.18 (n.s.)	0.05

The empirical correlation is strong, reproducible across seeds, and highly significant. Crucially it holds beyond the primary testbed: on Fashion-MNIST with a plain CNN (no residual connections) the log–log Pearson coefficient is -0.950 ± 0.017, an equally strong relationship to the -0.913 ± 0.013 measured on CIFAR-10/ResNet-18, and on Imagenette at real resolution it is -0.907 ± 0.021 with the standard full-stem ResNet-18, so the relation is neither an artefact of one network family nor of thumbnail-resolution inputs. This is the textbook quadratic relation $\alpha \approx 1/\lambda$ surviving into the deep-net regime in the sense made precise by Edge of Stability (Cohen et al., 2021): the line search is, in effect, a continuous online estimator of the same λ_1 that the EoS literature measures via expensive Lanczos iteration (Yao et al., 2020).

What does the line search actually invert? The correlation with λ_1 combines two facts: an exact, elementary one about backtracking, and a separate alignment fact borrowed from the Edge-of-Stability literature. Separating them shows what is ours and what is not. On a local quadratic model with Hessian $H \succ 0$, the backtracking line search along any descent direction d accepts a step α when $L(\theta + \alpha d) \le L(\theta) + c\,\alpha\, g^\top d$; expanding L to second order, this reduces to $\alpha \le 2(1-c)/q_d$ with the directional curvature

$$q_d \;=\; \frac{d^\top H d}{-\,g^\top d}$$

introduced above. Backtracking from $\alpha_{\max} = 1$ by factor β accepts the largest such β^k, so whenever the constraint binds the returned step obeys

$$\frac{q_d}{2(1-c)} \leq \frac{1}{\alpha} \leq \frac{q_d}{2\beta(1-c)}.$$

That is, the line search inverts the directional curvature q_d *along the probed direction*, not λ_1, up to the multiplicative backtracking band of width $1/\beta$. This exact statement is the part of the mechanism that is ours; which curvature it reports is then entirely a matter of which direction d one probes, and two choices matter.

The first is the *raw-gradient probe*, $d = -g$, for which $q_{-g} = g^\top Hg/\|g\|^2$ is the Rayleigh quotient of H along the gradient; we write q for q_{-g} in the measurement experiments that follow. This is the variant we use to expose the mechanism, because it admits a clean link to the top eigenvalue. We test the band directly by measuring α and q_{-g} on the *same* probe batch at each probe (a single extra Hessian-vector product). Across the CIFAR-10 and Fashion-MNIST mechanism runs, 73% of the probe points at which the Armijo constraint is active fall inside the predicted factor-2 band, with median ratio $(1/\alpha)/(q_{-g}/(2(1-c))) = 1.27$, comfortably inside the predicted $[1, 1/\beta] = [1, 2]$. The remaining $\approx 27\%$ sit just outside the band because α is quantised to powers of β and the mini-batch loss is only locally quadratic. The link to λ_1 is then the second, EoS-side fact: we measure $q_{-g} \approx 0.63\,\lambda_1$ (median over both architectures), i.e. the gradient carries a large but incomplete component along the top eigenvector, so $1/\alpha \approx q_{-g}/2 \approx 0.3\,\lambda_1$, a strong linear relation with a constant offset, exactly the parallel-but-below line seen in Figure 1. The novel, exact part of the mechanism is $1/\alpha \propto q_{-g}$; the proportionality $q_{-g} \propto \lambda_1$ is inherited from the Edge-of-Stability alignment phenomenon (Cohen et al., 2021; Damian et al., 2023).

The second choice is the one that makes the probe deployable. Adam does not step along $-g$; it steps along the preconditioned direction $d = -g/(\sqrt{v} + \epsilon) \approx -\operatorname{sign}(g)$. Probing along that direction measures q_d in the geometry the optimiser actually moves in: the curvature that matters is the curvature along the direction the optimiser actually takes. The payoff is concrete: the raw-gradient probe reports curvature in a coordinate system Adam never uses, so the safety factor that converts a probe reading into a step cap is architecture-specific, whereas the *Adam-direction probe* yields a single safety factor that transfers across networks unchanged. We establish this next, and it is what lets one probe-derived rule guard Adam across all the architectures we test.

Figure 1 visualises this within each architecture: $1/\alpha$ plotted against λ_1 on log–log scales follows a strong linear trend with fitted slopes of order one (1.46 on CIFAR-10, 1.06 on Fashion-MNIST, 1.02 on Imagenette), lying a roughly constant factor below the textbook $1/\alpha = \lambda_1$ reference, consistent with the $1/\alpha \approx 0.3\,\lambda_1$ estimate, a unit-slope law with a constant offset that the fitted slopes bracket (close on Fashion-MNIST, somewhat steeper on CIFAR-10).

The correlation above is a static snapshot; in practice the probe is useful because it tracks sharpness *online*. Figure 2 overlays, against the training step, the expensive top eigenvalue λ_1 (Lanczos), the directional curvature q, and the low-cost probe reading $1/\alpha$, for one run per architecture. The probe follows λ_1 throughout training (here a steady flattening, as the line search drives the iterate into lower-curvature regions) for about five forward passes per reading, against the k Hessian–vector products (each roughly two backward passes) that a Lanczos estimate of λ_1 needs. The reading has a floor: once the landscape is flat enough that the full step $\alpha = \alpha_{\max} = 1$ is accepted, $1/\alpha$ saturates at 1 and no longer resolves curvature below that level (visible on CIFAR-10 after $\sim$1000 steps). Where the Armijo constraint is active, though, the line-search step is a low-cost online sensor for local sharpness: a practical way to watch Edge-of-Stability dynamics without Hessian machinery.

How faithfully does the step read curvature, and what controls the fidelity? Table 2 characterises the probe as a sensor on the Fashion-MNIST CNN, where λ_1 is cheap and reliable to estimate (PyHessian/Lanczos) as a reference. Two knobs matter. The backtracking factor β sets the resolution: theory places $1/\alpha$ in $[q/2(1-c),\, q/2\beta(1-c)]$, a band of width $1/\beta$, and with the backtracking depth held fixed the reading tightens exactly as predicted, from a median $(1/\alpha)/(q/2)$ of 1.8 inside $[1, 2]$ at the default $\beta = 0.5$ to 1.07 inside $[1, 1.11]$ at $\beta = 0.9$, at the cost of proportionally more evaluations. The probe batch sets the noise: the relative standard deviation of the λ_1 and q estimates over independent batches falls from ≈ 0.4 at batch 64

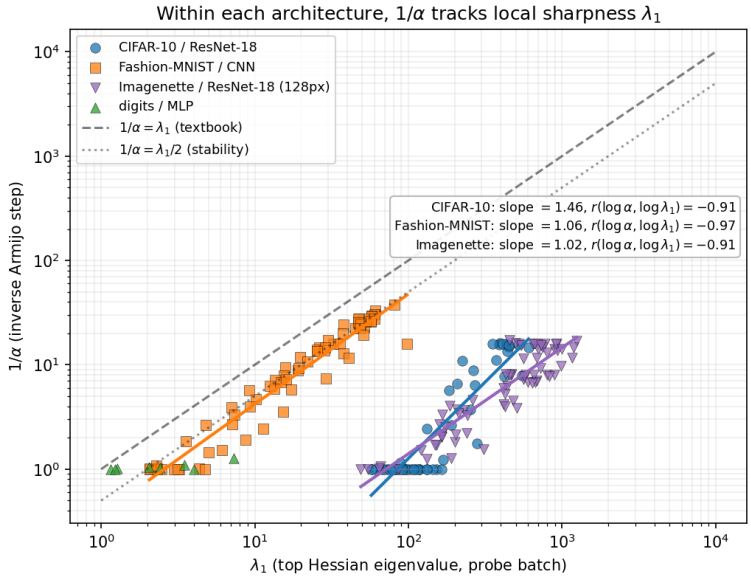

Figure 1: Within each architecture, $1/\alpha$ rises with λ_1 on log–log scales with fitted slopes 1.46 (CIFAR-10), 1.06 (Fashion-MNIST) and 1.02 (Imagenette) and strong correlation ($r = -0.91$, -0.97 and -0.91 between $\log \alpha$ and $\log \lambda_1$; the fits pool the three seeds of each architecture, per-seed statistics in Table 1), but lies a roughly constant factor *below* the textbook $1/\alpha = \lambda_1$ line (dashed), consistent with the step inverting the directional curvature $q \leq \lambda_1$ rather than λ_1 itself. The correlation is a within-run effect, so architectures are fitted separately and never pooled; digits (a small MLP whose λ_1 spans under a decade) is shown only as context.

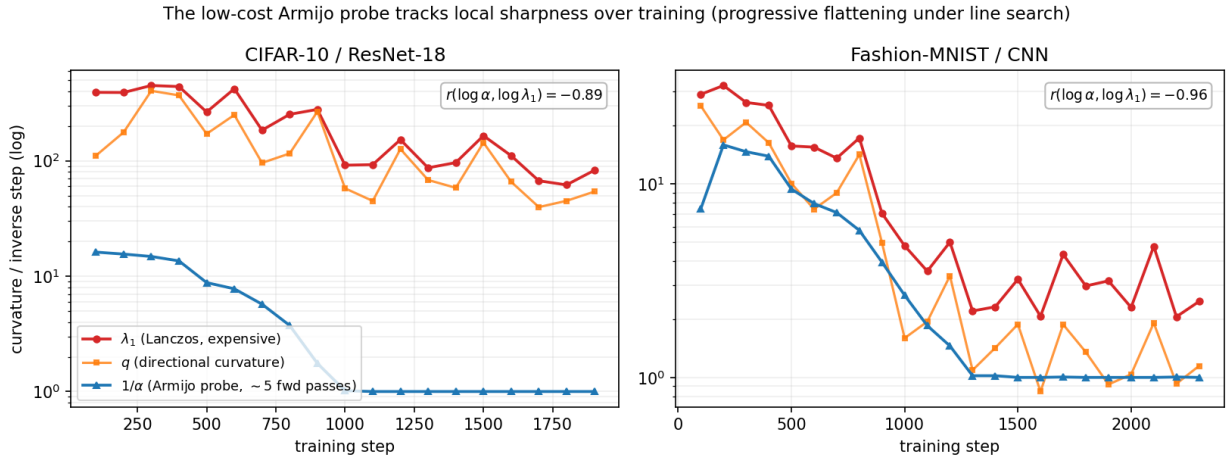

Figure 2: The low-cost Armijo probe tracks local sharpness over training. Per architecture (one run), the inverse line-search step $1/\alpha$ ($\sim$5 forward passes) follows the directional curvature q tightly and the Lanczos top eigenvalue λ_1 up to a constant factor, across the progressive flattening induced by the line search. $1/\alpha$ floors at 1 once the full step is accepted (CIFAR-10, late training), bounding the range it resolves.

to ≈ 0.1 at batch 256, so a few hundred examples already give a stable reading. Across these settings the directional curvature is a roughly constant fraction of the top eigenvalue, $q/\lambda_1 \approx 0.6$, matching the alignment used above.

Table 2: Fidelity of the line-search reading (Fashion-MNIST/CNN, 8 checkpoints). With the backtracking depth matched across β, the inverse step $1/\alpha$ reads the directional curvature q within the predicted band $[1, 1/\beta]$; a finer β tightens the band toward 1 at the cost of more evaluations. Probe-batch noise (λ_1/q relative std $0.4 \to 0.1$ from batch $64 \to 256$) and the $q \approx 0.6\,\lambda_1$ alignment are reported in the text.

backtracking factor β	predicted band $[1, 1/\beta]$	median $(1/\alpha)/(q/2)$ (% in band)
0.5 (default)	[1, 2.00]	1.79 (86%)
0.7	[1, 1.43]	1.23 (86%)
0.9	[1, 1.11]	1.07 (100%)

This establishes the paper's measurement claim: the line search reads local sharpness at low cost. We now turn to the practical pay-off: using that reading, once at initialisation, to cap a mis-specified learning rate. Table 3 reports test accuracy across the full lr range $\{10^{-3}, 10^{-2}, 10^{-1}, 0.3, 1.0, 3.0\}$ for vanilla Adam and the controllers, mean $\pm$ std over 5 seeds.

Table 3: CIFAR-10 / ResNet-18, 10 epochs. Test accuracy at six initial learning rates spanning more than three orders of magnitude. "DIV." = all seeds diverged at the first update (loss $\to$ NaN); "x/n div." = partial divergence with the surviving-seed mean. Mean $\pm$ std over five seeds; best per column within each block in bold.

η_{init}	10^{-3}	10^{-2}	10^{-1}	0.3	1.0	3.0
Vanilla Adam	$\mathbf{0.834 \pm 0.025}$	0.811 ± 0.016	DIV.	DIV.	DIV.	DIV.
Adam-InitOnly	0.833 ± 0.023	0.806 ± 0.016	$\mathbf{0.807 \pm 0.023}$	$\mathbf{0.799 \pm 0.026}$	$\mathbf{0.794 \pm 0.038}$	$\mathbf{0.796 \pm 0.023}$
Adam-Watchdog	0.808 ± 0.051	$\mathbf{0.816 \pm 0.020}$	0.797 ± 0.010	0.757 ± 0.010	0.233 (2/5 div.)	0.421 (3/5 div.)
Adam-Tracker	0.803 ± 0.023	0.766 ± 0.022	0.756 ± 0.027	0.765 ± 0.020	0.761 ± 0.026	0.772 ± 0.019
Direction-matched probe, fixed $\kappa = 2$ (no calibration)						
Adam-InitOnly (dir.)	$\mathbf{0.839 \pm 0.025}$	$\mathbf{0.823 \pm 0.016}$	$\mathbf{0.828 \pm 0.018}$	$\mathbf{0.824 \pm 0.024}$	$\mathbf{0.817 \pm 0.020}$	$\mathbf{0.823 \pm 0.023}$
Transfer check: AdamW base optimiser						
Vanilla AdamW	$\mathbf{0.843 \pm 0.014}$	0.809 ± 0.023	DIV.	DIV.	DIV.	DIV.
AdamW-InitOnly (dir.)	0.828 ± 0.029	$\mathbf{0.823 \pm 0.016}$	$\mathbf{0.827 \pm 0.019}$	$\mathbf{0.816 \pm 0.018}$	$\mathbf{0.818 \pm 0.019}$	$\mathbf{0.826 \pm 0.020}$
Parameter-free / schedule-free baselines (no κ; η swept like the rest)						
Schedule-Free AdamW	$\mathbf{0.865 \pm 0.005}$	$\mathbf{0.864 \pm 0.006}$	DIV.	DIV.	DIV.	DIV.
Prodigy	0.100 ± 0.005	0.529 ± 0.003	$\mathbf{0.768 \pm 0.006}$	$\mathbf{0.795 \pm 0.011}$	$\mathbf{0.813 \pm 0.010}$	$\mathbf{0.827 \pm 0.018}$

Vanilla Adam is competitive at the optimal $\eta = 10^{-3}$ (0.834) but diverges in the very first step at any $\eta \geq 10^{-1}$; the watchdog absorbs one further decade of misspecification before failing, and the tracker survives the whole range at a persistent accuracy cost (Figure 3). The most informative row is the simplest one. Adam-InitOnly, which performs only the calibration probe before the first Adam step and then leaves Adam entirely alone, matches vanilla Adam at the optimal η (0.833 vs 0.834, within seed noise) and stays in $[0.79, 0.83]$ across the full range. It matches or exceeds Adam-Tracker at every learning rate, has no periodic compute overhead, and, as the transfer experiments below show, is the only controller whose settings carry over to other architectures. We recommend Adam-InitOnly as the practical default.

The fair comparison is not vanilla Adam at an arbitrary learning rate (which no practitioner would deliberately choose) but vanilla Adam whose η has been *tuned*, typically by a learning-rate sweep or range test (Smith, 2017). Adam-InitOnly delivers essentially that tuned accuracy without the search: its worst cell over the entire range (0.794 at $\eta = 1.0$) is within five percent of optimally-tuned vanilla Adam's best (0.834 at $\eta = 10^{-3}$), and it reaches this from a single probe at *every* learning rate. We make this comparison concrete in Table 4: against an actual learning-rate range test (Smith, 2017) that ramps η over ~ 2 epochs and then trains at the rate it finds, the one-shot probe (given a deliberately too-large $\eta = 0.1$ to cap) reaches the same or slightly better test accuracy (0.822 vs 0.792, 3 seeds, both with zero divergences) for the cost of a single ~ 50 ms probe rather than the range test's ~ 2 ramp epochs. The probe is therefore best read not as beating a

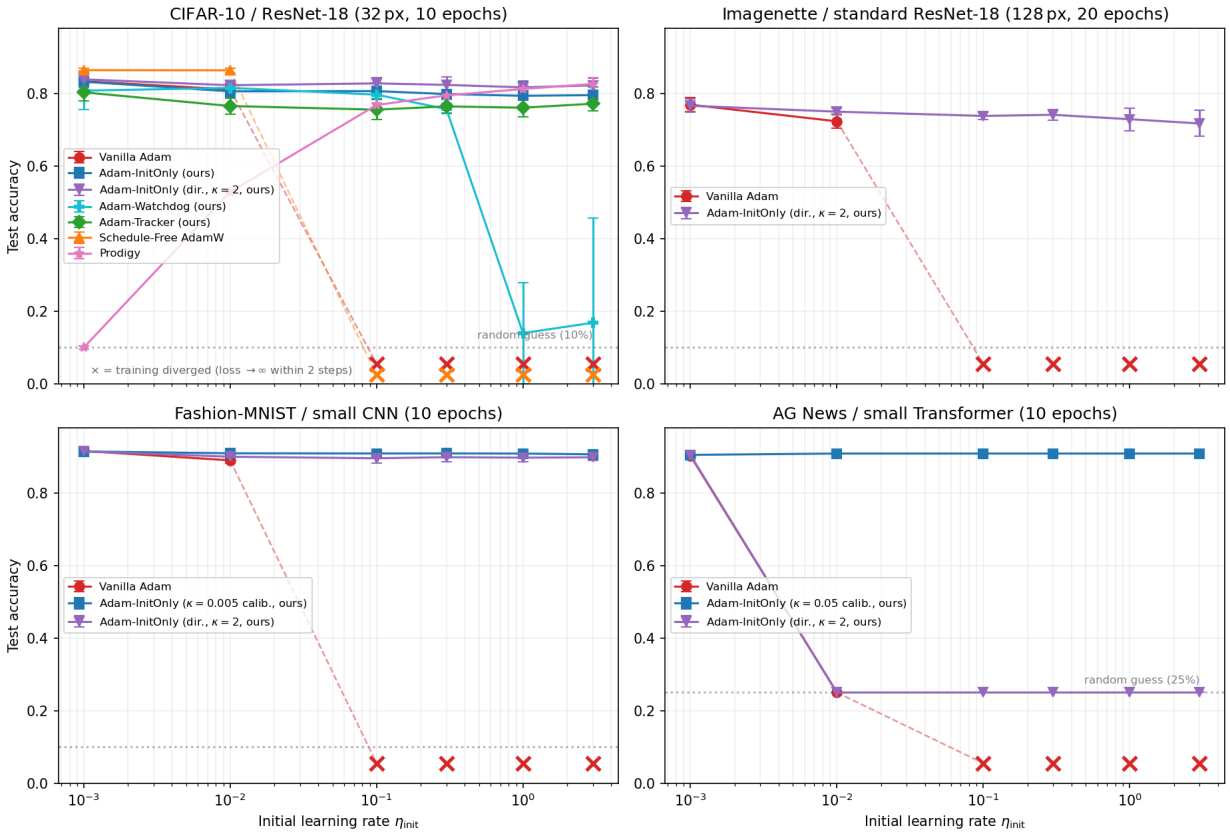

Figure 3: Test accuracy vs. initial learning rate, mean±std over five seeds; "×" markers at the bottom mark runs that diverged (loss $\to \infty$ within two steps), with a dashed "cliff" joining each diverging method to its last surviving point; dotted grey lines mark random-guess accuracy. *Top left:* CIFAR-10/ResNet-18, all methods. Vanilla Adam (red) and Schedule-Free AdamW (orange) fall off the cliff for $\eta \geq 10^{-1}$, the parameter-free baselines each cover only part of the range, and the calibrated Adam-InitOnly (blue) and the calibration-free direction-matched variant at the fixed $\kappa = 2$ (purple) stay near-optimal across all six rates. *Top right:* the real-resolution Imagenette control (standard full-stem ResNet-18 at 128px) repeats the pattern with the same fixed $\kappa = 2$. *Bottom left:* Fashion-MNIST, where the calibrated raw-gradient probe ($\kappa = 0.005$) and the calibration-free $\kappa = 2$ coincide. *Bottom right:* AG News makes the limit of the calibration-free recipe visible: the fixed $\kappa = 2$ still prevents every divergence but settles on the random-guess plateau for $\eta \geq 10^{-2}$, while the one-minute calibration ($\kappa = 0.05$) recovers full accuracy.

deliberately broken baseline, but as approximating the *safety* role of a coarse learning-rate sweep at a fraction of its cost. The probe targets the safety role of a range test rather than the search for a performance-optimal rate, and it occupies that role for the cost of one probe.

Table 4: A real learning-rate range test versus the one-shot probe, on CIFAR-10/ResNet-18, mean over 3 seeds. The range test ramps η over $\sim$2 epochs and trains at the learning rate it finds; Adam-InitOnly is handed a deliberately too-large $\eta = 0.1$ and caps it with a single init probe. Both avoid divergence; the probe matches the sweep's safety, here at slightly higher accuracy, for a fraction of the cost.

Method	effective η	test acc	extra cost	div.
LR range test (Smith) $\rightarrow$ train	0.018	0.792	$\sim$2 epochs (ramp)	0/3
Adam-InitOnly (probe @ $\eta = 0.1$)	0.016	**0.822**	$\sim$1 probe ($\sim$50 ms)	0/3

Modern parameter-free optimisers do not remove the need for this safeguard. The last two rows of Table 3 report two recent parameter-free / schedule-free optimisers run across the same grid: Schedule-Free AdamW (Defazio et al., 2024) and Prodigy (Mishchenko & Defazio, 2024).[1] Neither covers the full range. Schedule-Free AdamW is strongest of all at small η (0.865/0.864 at $\eta \leq 10^{-2}$, above every other method) but still diverges in the first step for any $\eta \geq 10^{-1}$, exactly the failure our probe targets. Prodigy never diverges, but its internal step-size estimate starts far too small at $\eta = 10^{-3}$ (test accuracy at random-guess level) and only becomes competitive once $\eta \geq 10^{-1}$, where it is in fact the best method (0.813/0.827 at $\eta = 1.0/3.0$). Each parameter-free optimiser thus excels in a different part of the range but collapses at the opposite end, whereas Adam-InitOnly stays within about four percentage points of its own optimum across the entire 10^{-3}–3.0 range with no divergence; the probe is a calibrate-once safety check for Adam, not a competing optimiser, and these results are complementary rather than contradictory.

The direction-matched block of Table 3 removes even the one-time calibration: at the single fixed $\kappa = 2$, the direction-matched probe matches the calibrated raw-gradient variant across the entire grid (0.82–0.84, zero divergences), with no per-architecture sweep at all. The AdamW block repeats the experiment with the base optimiser swapped: vanilla AdamW diverges from $\eta = 0.1$ exactly like Adam, and the identical probe at the identical κ restores the full range.

Figure 4 shows the $\eta = 10^{-1}$ case explicitly: vanilla Adam's loss explodes within two steps and is irrecoverable, while Adam-InitOnly and the two periodic controllers all train normally. Figure 5 shows what the controllers actually do with η: the rescue is done up front by the init probe, which caps the requested $\eta = 0.1$ down to ≈ 0.016 before the first update. From there the two periodic controllers *relax* the rate rather than throttle it further: the watchdog climbs back to the user's 0.1 ceiling and holds, while the tracker follows the probed step size up to ≈ 0.25. The rescue is therefore attributable to the one-shot cap, not to continued shrinking during training, which is precisely why the init probe alone suffices.

A reasonable concern is that the rescue effect is also achieved by simpler standard tricks. Table 5 compares the controllers against gradient norm clipping ($\|g\| \leq 1.0$) and a 200-step linear warmup at the two diagnostic learning rates $\eta = 10^{-1}$ and $\eta = 1.0$.

The two low-cost baselines are revealing in different ways. Global gradient-norm clipping at $\|g\| \leq 1$ leaves vanilla Adam essentially unchanged at well-tuned learning rates (0.836 ± 0.021 at $\eta = 10^{-3}$ against vanilla Adam's 0.834 ± 0.025, identical within seed noise), so the clip neither helps nor hurts there. At misspecified learning rates it provides no rescue at all: Adam still diverges in the first step at $\eta = 10^{-1}$ and at $\eta = 1.0$. The reason is structural rather than numerical. Adam's update is $\eta\, m_t/(\sqrt{v_t} + \varepsilon)$, and during the first few steps v_t is initialised at zero and the $1/\sqrt{v_t}$ factor amplifies even a clipped gradient by orders of magnitude; clipping the gradient *before* this amplification has limited effect on the resulting parameter update. Linear warmup performs better but only partially: it absorbs $\eta = 10^{-1}$ at accuracy on par with the init probe (0.809 ± 0.028 vs 0.807 ± 0.023), but at $\eta = 1.0$ the warmup target is itself unstable, with three of five seeds diverging and the surviving seeds settling at the random-guess level. Of the probe-based controllers, both Adam-InitOnly

[1] Prodigy is normally run at its default multiplier $\eta = 1.0$, where it indeed performs well here; we sweep the multiplier like every other method because our question is precisely how each method behaves when the user-specified scale is wrong.

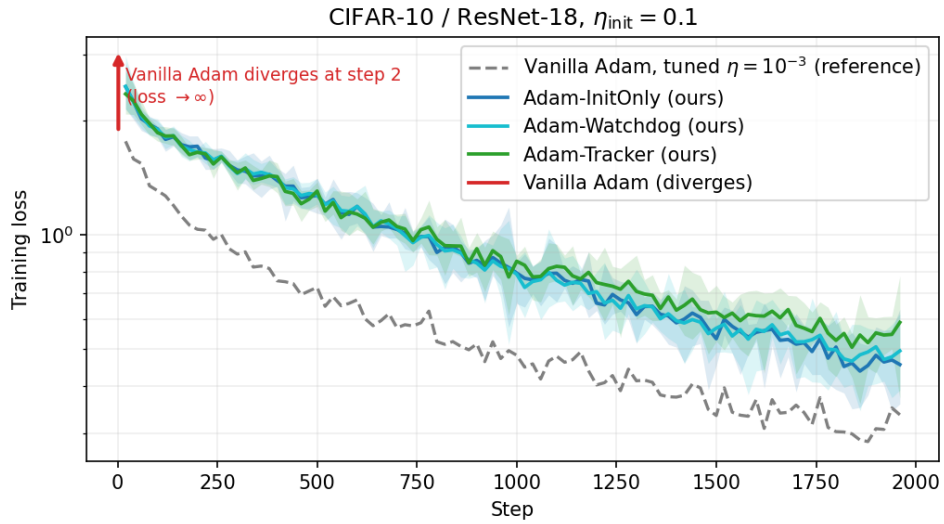

Figure 4: Training loss at the misspecified $\eta_{\text{init}} = 0.1$ (mean over 5 seeds, shaded min–max). The grey dashed reference is vanilla Adam at its well-tuned $\eta = 10^{-3}$, which trains normally: Adam is not failing at CIFAR-10, only at this 100×-too-large rate. At $\eta = 0.1$ vanilla Adam instead diverges at step 2 (loss $\to \infty$, off chart), whereas Adam-InitOnly and the two periodic controllers train fine and approach the tuned reference, all from the same bad η_{init}.

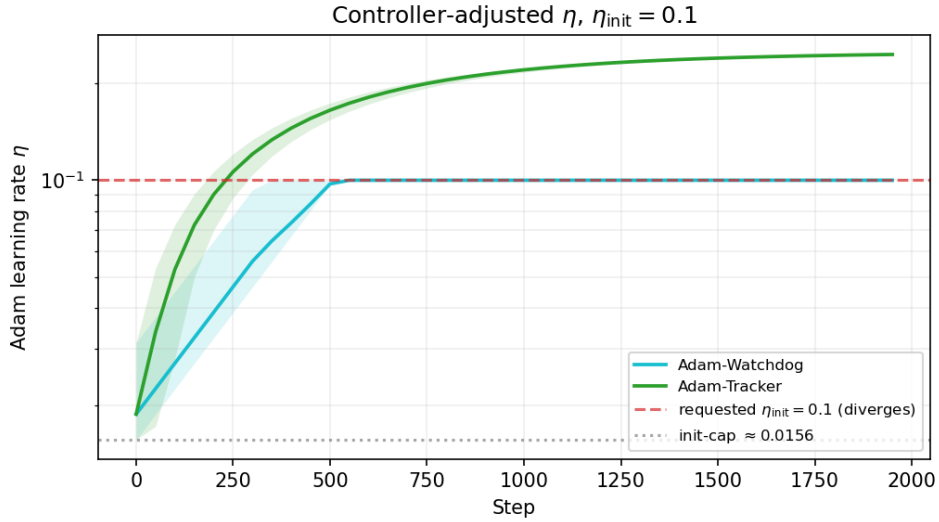

Figure 5: Controller-adjusted η at $\eta_{\text{init}} = 0.1$ (mean over 5 seeds, shaded min–max). The init probe caps the requested $\eta = 0.1$ to ≈ 0.016 before training (dotted); the watchdog then relaxes η back to the user's 0.1 ceiling, while the tracker follows the probed step size up to ≈ 0.25.

Table 5: Comparison of the probe controllers with low-cost standard baselines (gradient-norm clipping, linear warmup) at a well-tuned ($\eta = 10^{-3}$) and two misspecified ($\eta = 10^{-1}, 1.0$) initial learning rates; CIFAR-10/ResNet-18, mean±std over five seeds; best per column within each block in bold. "DIV." = all seeds diverged at the first update; "x/n div." = partial divergence (surviving-seed mean).

	$\eta_{\text{init}} = 10^{-3}$	$\eta_{\text{init}} = 10^{-1}$	$\eta_{\text{init}} = 1.0$
Vanilla Adam and standard defences			
Vanilla Adam	0.834 ± 0.025	DIV.	DIV.
Adam + grad-clip ($\|g\| \leq 1$)	$\mathbf{0.836 \pm 0.021}$	DIV.	DIV.
Adam + 200-step warmup	0.835 ± 0.015	$\mathbf{0.809 \pm 0.028}$	0.10^{*} (3/5 div.)
Probe-based controllers (ours)			
Adam-InitOnly	$\mathbf{0.833 \pm 0.023}$	$\mathbf{0.807 \pm 0.023}$	$\mathbf{0.794 \pm 0.038}$
Adam-Watchdog	0.808 ± 0.051	0.797 ± 0.010	0.233 (2/5 div.)
Adam-Tracker	0.803 ± 0.023	0.756 ± 0.027	0.761 ± 0.026

[*] Surviving seeds failed to learn; test accuracy at random-guess level.

and Adam-Tracker survive every tested learning rate up to $\eta = 3.0$ (Table 3), whereas Adam-Watchdog fails from $\eta = 1.0$ on; Adam-InitOnly does so at the higher accuracy and, as we show next, is the only one whose single setting also transfers to a second architecture.

A single architecture is not enough to trust the recipe, so we now ask whether the controller settings transfer. To test this, we ran the same sweep on the Fashion-MNIST CNN, with the same default $\kappa = 0.25$ and watchdog thresholds calibrated on CIFAR-10. Five seeds per cell. The result is reported in the upper block of Table 6, alongside the calibrated version discussed below.

Inspecting the controller logs reveals two distinct failures: *(i)* On Fashion-MNIST the probe saturates: the Armijo condition already holds at the full step, so $\bar{\alpha}_{\text{init}} = 1$, unlike on CIFAR-10, where backtracking engages and returns $\bar{\alpha}_{\text{init}} \approx 0.06$. At the same time the largest *stable* Adam learning rate on Fashion-MNIST/small-CNN is only ≈ 0.01 (cf. vanilla Adam's divergence at $\eta = 0.1$), so the stable fraction of the probed step is ≈ 0.01 here against ≈ 0.3 on CIFAR-10; the conversion factor κ must therefore absorb a gap of well over an order of magnitude. The default safety factor $\kappa = 0.25$ caps η at 0.25, far above the stable range: at $\eta = 0.1$ the cap does not engage at all, and at the larger requested rates it does engage but only reduces them to 0.25, which is itself still unstable, so the init-probe rescue cannot help here. *(ii)* On the small CNN, sharpness rises much faster in the first hundred steps (progressive sharpening is more violent on a small network), so α collapses from 1 to ≈ 0.008 within 100 steps. Watchdog interprets this as a divergence signal and shrinks η from 0.001 to its floor 5×10^{-5}, well below the optimum.

The fix follows directly from this diagnosis, and it makes the recipe simpler rather than more complex. We re-ran the same Fashion-MNIST sweep with κ recalibrated to the architecture: the largest stable vanilla-Adam learning rate is $\approx 10^{-2}$ (cf. the upper block of Table 6), and $\bar{\alpha}_{\text{init}} \approx 1$, so we pick $\kappa = 0.005$ (half of the empirical stability boundary).

The result is unambiguous: with one-time calibration of κ, Adam-InitOnly yields test accuracy 0.91 ± 0.005 across *all* six learning rates, 5 seeds each, with zero divergences. This mirrors and even strengthens the CIFAR-10 rescue result: across more than three orders of magnitude of misspecification (10^{-3} to 3.0), test accuracy drops by less than 1 percentage point relative to the optimal vanilla-Adam configuration. The direction-matched probe achieves the same without the sweep (final block; Figure 3, bottom left): 0.90–0.91 across all six rates, zero divergences, at the fixed $\kappa = 2$. The two parameter-free baselines (last block of Table 6) again cover only part of the range: Schedule-Free AdamW is the strongest method at $\eta \leq 10^{-2}$ but diverges for $\eta \geq 10^{-1}$, while Prodigy is robust from 10^{-2} to 3.0 yet collapses to random-guess accuracy at $\eta = 10^{-3}$. The two failure modes are complementary and opposite, and neither matches the calibrated init probe's coverage of all six rates.

The simpler controller wins here for a structural reason. The Watchdog and Tracker modes were tuned on CIFAR-10/ResNet-18, where progressive sharpening (Cohen et al., 2021) is comparatively gentle and the

Table 6: Fashion-MNIST rescue: uncalibrated $\kappa = 0.25$ versus calibrated $\kappa = 0.005$. Mean±std over 5 seeds; best per column within each block in bold. "DIV." = all 5 seeds diverged; "(x/n)" = x of n seeds diverged, surviving-seed mean shown. * surviving seeds learned nothing.

η_{init}	10^{-3}	10^{-2}	10^{-1}	0.3	1.0	3.0
Uncalibrated, $\kappa = 0.25$ (CIFAR-10 default)						
Vanilla Adam	0.916 ± 0.003	0.890 ± 0.008	DIV.	DIV.	DIV.	DIV.
Adam + grad-clip	$\mathbf{0.917 \pm 0.002}$	0.899 ± 0.004	DIV.	DIV.	DIV.	DIV.
Adam + warmup	0.913 ± 0.004	$\mathbf{0.903 \pm 0.003}$	DIV.	0.10* (2/5)	0.10*	DIV.
Adam-Watchdog	0.878 ± 0.002	0.889 ± 0.013	DIV.	DIV.	DIV.	DIV.
Adam-Tracker	0.81 (3/5)	0.10* (4/5)	DIV.	DIV.	DIV.	DIV.
Calibrated, $\kappa = 0.005$ (one extra divergence sweep, <1 minute)						
Adam-InitOnly	$\mathbf{0.914 \pm 0.005}$	$\mathbf{0.909 \pm 0.004}$	$\mathbf{0.909 \pm 0.004}$	$\mathbf{0.909 \pm 0.004}$	$\mathbf{0.908 \pm 0.003}$	$\mathbf{0.907 \pm 0.003}$
Adam-Watchdog	0.878 ± 0.002	$\mathbf{0.909 \pm 0.005}$	$\mathbf{0.909 \pm 0.004}$	0.895 ± 0.004	0.65 (1/5)	0.10* (4/5)
Adam-Tracker	DIV.	0.46 (3/5)	0.10* (4/5)	0.84 (4/5)	0.10* (3/5)	DIV.
Direction-matched probe, fixed $\kappa = 2$ (no calibration)						
Adam-InitOnly (dir.)	$\mathbf{0.914 \pm 0.004}$	$\mathbf{0.900 \pm 0.005}$	$\mathbf{0.896 \pm 0.015}$	$\mathbf{0.899 \pm 0.014}$	$\mathbf{0.897 \pm 0.012}$	$\mathbf{0.898 \pm 0.010}$
Parameter-free / schedule-free baselines (no κ)						
Schedule-Free AdamW	$\mathbf{0.914 \pm 0.001}$	$\mathbf{0.920 \pm 0.002}$	DIV.	DIV.	DIV.	DIV.
Prodigy	0.102 ± 0.046	0.876 ± 0.002	$\mathbf{0.915 \pm 0.004}$	$\mathbf{0.917 \pm 0.002}$	$\mathbf{0.911 \pm 0.006}$	$\mathbf{0.910 \pm 0.009}$

periodic adjustments tracked the curvature dynamics usefully. On a small CNN with stronger progressive sharpening, the same periodic adjustments overshoot: the Watchdog shrinks η down to its floor of $0.05\,\eta_{\text{init}}$, the Tracker EMA pulls η outside the stable range. Removing the periodic component (Adam-InitOnly) lets Adam's own adaptive $1/\sqrt{v_t}$ scaling handle in-training curvature changes, and performs strictly better. This sharpens the recommendation: the init probe is the primary mechanism, and periodic probing is at most a safety net that requires its own per-architecture tuning.

This calibration is low-cost. The extra cost of fixing κ to a new architecture is a single divergence sweep like the one in Appendix C (~ 50 Adam runs of ≤ 1 epoch each), or roughly one minute on the hardware of Section 4. Once calibrated, Adam-InitOnly deploys with $<2\%$ wall-clock overhead per training run.

To test whether the recipe extends beyond vision, we repeat the study on the text benchmark: AG News with the small Transformer. The probe and controllers are unchanged; results over the same 6×5 grid are in Table 7.

The pattern mirrors Fashion-MNIST closely. With the CIFAR default $\kappa = 0.25$, no method is robust: vanilla Adam, Adam-InitOnly and Adam-Watchdog all collapse to random-guess accuracy the moment $\eta \geq 10^{-2}$, because the largest stable Adam learning rate on this Transformer is only $\approx 3 \times 10^{-3}$ and the probe's safe-step estimate at initialisation ($\bar{\alpha}_{\text{init}} \approx 0.031$) caps η at $0.25\,\bar{\alpha}_{\text{init}} \approx 8 \times 10^{-3}$, still above the stable range. The two parameter-free baselines again cover only part of the grid: Schedule-Free AdamW fails for $\eta \geq 10^{-2}$, and Prodigy is robust only in a middle band (10^{-2} to 0.3) while failing at both ends. After the divergence sweep sets $\kappa = 0.05$, Adam-InitOnly recovers 0.905–0.909 across all six learning rates, more than three orders of magnitude of misspecification, with zero divergences. The periodic controllers do not transfer even after recalibration, confirming that the one-shot init probe, not the periodic machinery, is the component that generalises across domains.

The direction-matched probe marks the limit of the calibration-free recipe here (final block of Table 7; Figure 3, bottom right). At the fixed $\kappa = 2$ it still prevents every divergence, but on this Transformer, whose stable range is unusually narrow ($\eta \approx 10^{-3}$), the uncalibrated cap lands in the stable-yet-unproductive band, and the runs sit at chance for $\eta \geq 10^{-2}$. Where the stable range is that narrow, the fixed cap is a divergence safeguard only; the calibration sweep is what turns it into a full rescue.

Imagenette, the real-resolution control of Section 4, completes the transfer picture. Vanilla Adam repeats the CIFAR-10 pattern exactly, competitive at $\eta = 10^{-3}$ and diverging in the first step from $\eta = 0.1$ on, and the fixed $\kappa = 2$ again removes every divergence while staying within about five points of the tuned optimum

Table 7: AG News / small Transformer: uncalibrated $\kappa = 0.25$ versus calibrated $\kappa = 0.05$. Mean±std over 5 seeds; best per column within each block in bold. "DIV." = all seeds diverged (loss → NaN); a bare 0.250 is random-guess accuracy (4 balanced classes), i.e. the run was stable but failed to learn; "x/n div." = partial divergence with surviving-seed mean. The optimal vanilla-Adam learning rate here is $\eta \approx 10^{-3}$, two orders of magnitude tighter than on CIFAR-10, so the CIFAR default $\kappa = 0.25$ caps the learning rate above the stable range and does not rescue, exactly as on Fashion-MNIST. A one-minute divergence sweep gives $\kappa = 0.05$, after which Adam-InitOnly is robust across all six rates.

η_{init}	10^{-3}	10^{-2}	10^{-1}	0.3	1.0	3.0
Uncalibrated, $\kappa = 0.25$ (CIFAR-10 default)						
Vanilla Adam	0.902 ± 0.003	0.250	DIV.	DIV.	DIV.	DIV.
Adam-InitOnly	$\mathbf{0.905 \pm 0.003}$	0.250	0.250	0.250	0.250	0.250
Adam-Watchdog	0.904 ± 0.002	0.250	0.250	DIV.	DIV.	DIV.
Adam-Tracker	DIV.	DIV.	DIV.	DIV.	DIV.	DIV.
Schedule-Free AdamW	0.903 ± 0.003	0.251	0.250 (3/5 div.)	DIV.	DIV.	DIV.
Prodigy	0.232 ± 0.007	$\mathbf{0.880 \pm 0.002}$	$\mathbf{0.906 \pm 0.002}$	$\mathbf{0.908 \pm 0.002}$	0.408 ± 0.195	0.259 ± 0.018
Calibrated, $\kappa = 0.05$ (one extra divergence sweep, <1 minute)						
Adam-InitOnly	$\mathbf{0.905 \pm 0.003}$	$\mathbf{0.909 \pm 0.002}$	$\mathbf{0.909 \pm 0.002}$	$\mathbf{0.909 \pm 0.002}$	$\mathbf{0.909 \pm 0.002}$	$\mathbf{0.909 \pm 0.002}$
Adam-Watchdog	0.904 ± 0.002	0.250	0.250	DIV.	DIV.	DIV.
Adam-Tracker	DIV.	DIV.	DIV.	DIV.	DIV.	DIV.
Direction-matched probe, fixed $\kappa = 2$ (no calibration)						
Adam-InitOnly (dir.)	$\mathbf{0.904 \pm 0.003}$	0.250	0.250	0.250	0.250	0.250

(Figure 3, top right; exact numbers in Appendix F). The rescue thus carries over from thumbnails to real images and to the unmodified stem.

A sharper test is the case where the default learning rate is itself unsafe. On every benchmark above the Adam framework default $\eta = 10^{-3}$ lies in the stable range, so the init cap never fires and training is untouched. Its value appears only where the default is genuinely too large for the curvature at initialisation. Two well-known such regimes are normalisation-free networks and warmup-free deep Transformers (Table 8): a ResNet-18 with all normalisation removed on CIFAR-10, and a deeper 12-layer variant of the AG News Transformer (versus the 4-layer model used above) trained without warmup. At the default $\eta = 10^{-3}$ vanilla Adam *diverges* (no-normalisation ResNet, all seeds) or *collapses to chance* (warmup-free Transformer); Adam-InitOnly, with κ recalibrated by the same sweep, caps the rate into the stable range and recovers accuracy within a point or two of the best tuned vanilla Adam, without the user knowing the safe rate in advance. The caveat is that the CIFAR default $\kappa = 0.25$ does not transfer to these higher-curvature settings (it still diverges). Together with the CIFAR-10 grid, these results establish the paper's rescue claim: the one-shot cap rescues where the default rate is genuinely unsafe and is a no-op otherwise.

Table 8: Where the default learning rate is itself unsafe. At Adam's framework default $\eta = 10^{-3}$, a normalisation-free ResNet and a warmup-free deep Transformer diverge or fail to learn; the one-shot init cap (with a per-architecture κ, set by a one-minute divergence sweep) recovers accuracy within a point or two of the best tuned vanilla Adam, whereas the default $\kappa = 0.25$ does not transfer. Mean over 4 seeds; short protocol (ResNet 3 epochs, Transformer 600 steps).

Setting	vanilla, default 10^{-3}	vanilla, best tuned	Adam-InitOnly @ 10^{-3}
ResNet-18, *no normalisation* (CIFAR-10)	DIV. (4/4)	0.537 (η=3×10^{-4})	0.535 (κ=0.05)
Transformer, *no warmup* (AG News)	0.250 (chance)	0.828 (η=3×10^{-4})	0.810 (κ=0.005)

Two further checks (the empirical divergence boundary that fixes κ, and a 100-epoch cosine schedule on which the rescued runs retain their full $\approx 93\%$ accuracy across the entire grid) are deferred to Appendices C and D.

The rescues above each used a per-architecture κ, set by a one-minute divergence sweep, and this is their main practical drawback. It is, however, a property of the *probed direction*, not of the method, and the direction-matched probe removes it. The plain-gradient probe reports $\bar{\alpha}_{\text{init}}$ in a coordinate system Adam never steps in, so the conversion factor that κ must absorb depends on the per-architecture gradient scale.

Probing instead along Adam's own preconditioned direction $-g/(\sqrt{v}+\varepsilon) \approx -\operatorname{sign}(g)$ returns $\bar{\alpha}_{\text{init}}$ in the geometry Adam actually moves in, and that dependence disappears. Table 9 confirms it. A single fixed $\kappa = 3$, chosen on four architectures and held out on five unseen ones, caps safely across nine architectures (BatchNorm, GroupNorm and normalisation-free nets; a plain MLP; an LSTM; CNNs and Transformers of several scales) and two learning rates: 2 divergences in 54 runs, against 10 for the plain-gradient probe at a single κ and 22 for vanilla Adam, and *zero* at the framework default. Both failures occur on a plain MLP at the 100×-too-large rate, and a sweep of the safety factor (Table 10) removes them: $\kappa = 2$ and even $\kappa = 1$ give zero divergences in all 54 runs at no accuracy cost, so we recommend $\kappa = 2$ as the less intrusive of the two divergence-free settings. Accuracy tells the same story (Table 9, lower block): counting a divergent run as zero, the direction-matched probe reaches a mean of 0.73/0.63 at the default/100× rate, against 0.59/0.09 for vanilla Adam and 0.55/0.29 for the plain-gradient probe. Because the nine architectures have different chance levels and task difficulties, Figure 6 breaks the discriminating 100× rate down per architecture: at $\kappa = 2$ the direction-matched probe is the most accurate variant on each and diverges on none (exact numbers in Appendix E). The full learning-rate grids extend this beyond the two spot rates: at the same fixed $\kappa = 2$ the direction-matched probe diverges nowhere up to $\eta = 3.0$ on all four benchmarks, with full accuracy recovery on CIFAR-10, Fashion-MNIST and Imagenette (Appendix F) and the AG News limit discussed above (final blocks of Tables 3, 6 and 7). The same recipe also transfers to AdamW unchanged (AdamW block of Table 3). The per-architecture κ of the body experiments, which predate this fix, is thus a limitation of the gradient-direction probe rather than of the safeguard itself.

Table 9: A single, architecture-independent safety factor. Divergent runs and mean test accuracy over nine architectures × {default $\eta = 10^{-3}$, 100× too large} × 3 seeds. Probing along Adam's preconditioned direction lets one fixed $\kappa = 3$ cap safely almost everywhere (with zero divergences at the default rate), whereas the plain-gradient probe needs a per-architecture κ. Accuracy counts a divergent run as 0, so it rewards both not diverging and still learning; the direction-matched probe is best on both rows. Both direction-matched failures occur on a plain MLP at the 100× rate.

	vanilla Adam	plain-grad probe ($\kappa = 0.25$)	Adam-direction probe ($\kappa = 3$)
Divergent runs			
at default $\eta = 10^{-3}$ (of 27)	1	2	**0**
at 100× too large (of 27)	21	8	**2**
total (of 54)	22	10	**2**
Mean test accuracy (divergent run = 0)			
at default $\eta = 10^{-3}$	0.586	0.548	**0.730**
at 100× too large	0.089	0.292	**0.631**

Table 10: Sweeping the safety factor of the Adam-direction probe over the same nine architectures × two rates × three seeds. A more conservative κ removes the last divergences with a favourable accuracy trade-off: $\kappa = 2$ and $\kappa = 1$ give zero divergences in all 54 runs. The small drop at the default rate (0.703 for $\kappa = 2$ vs. 0.730 for $\kappa = 3$) is outweighed by the much higher accuracy at the 100× rate (0.733 vs. 0.631), where $\kappa = 3$ also diverges twice. We recommend $\kappa = 2$.

Adam-direction probe	$\kappa = 1$	$\kappa = 2$	$\kappa = 3$
divergences at default 10^{-3} (of 27)	**0**	**0**	0
divergences at 100× (of 27)	**0**	**0**	2
total divergences (of 54)	**0**	**0**	2
mean acc at default 10^{-3}	0.728	0.703	0.730
mean acc at 100×	**0.737**	0.733	0.631

Finally we turn to cost. Wall-clock overhead in our setting is dominated by the explicit Hessian probes used to measure the α–λ_1 correlation above; the probes are an instrumentation artefact and are not part of the deployed controller. We report the two sets separately. With Hessian probes turned on, vanilla Adam takes

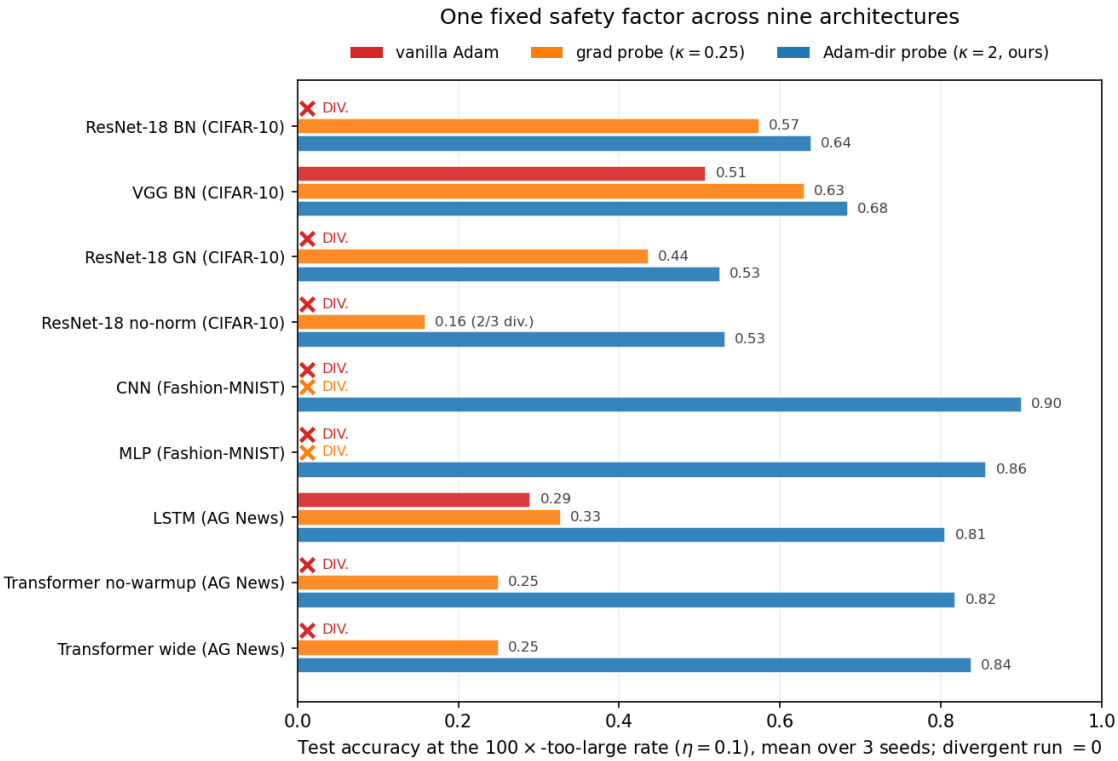

Figure 6: The transfer result at a glance: per-architecture test accuracy at the 100×-too-large learning rate ($\eta = 0.1$; mean over 3 seeds, divergent run counted as 0). With a single fixed safety factor, the direction-matched probe ($\kappa = 2$, blue) trains on all nine architectures and is the most accurate variant on each, whereas vanilla Adam (red) diverges on seven of the nine and the plain-gradient probe at one fixed $\kappa = 0.25$ (orange) diverges on two and degrades on others. Exact values in Table 15.

73.1 seconds for ten CIFAR-10 epochs, Adam-Tracker takes 76.1 seconds (+4%), and Adam-Watchdog takes 80.4 seconds (+10%); the difference is the extra forward and forward-backward passes the periodic Armijo probe performs. With Hessian probes turned off (the deployed configuration), the cost depends on how often the controller probes. Adam-InitOnly probes once, at initialisation: one extra forward-and-backward pass plus a handful of forward-only backtracks, an overhead of about 1% that is within measurement noise of vanilla Adam. The periodic controllers cost more. In a controlled interleaved benchmark (3 seeds, single session, GPU warmed up) over ten CIFAR-10 epochs, vanilla Adam takes 56.9 s; Adam-Tracker adds +2.7% and Adam-Watchdog +5.3%. These figures use forward-only backtracking; recomputing a gradient at every backtracking trial (the naive implementation) roughly doubles the periodic overhead, with Adam-Watchdog rising from +5.3% to +12.0%, which is why the probe evaluates the trial loss without a backward pass.

Several limitations bound these claims. The first, the per-architecture κ of the plain-gradient probe, was addressed above: it is a property of the probed direction, and the direction-matched probe removes it.

A second limitation, related to the first, is the fragility of the periodic-probe controllers under rapid progressive sharpening: on the small CNN their pre-tuned thresholds and EMA constants overshoot the true sharpness boundary, and even after κ is recalibrated both underperform Adam-InitOnly. We accordingly keep Watchdog and Tracker as opt-in features for users who want continuous in-training adaptation.

To quantify this, we compared the periodic Tracker across regimes at the framework default $\eta = 10^{-3}$ (Table 11). On well-conditioned real tasks its step-size growth overshoots and *hurts*: it loses several accuracy points on CIFAR-10/ResNet-18 and diverges on the AG-News Transformer (5/5 seeds), at *every* probe interval K we tried, so the failure is intrinsic to raising the rate on a smooth landscape rather than a matter of tuning K. On a plateau-dominated toy (a 2-2 XOR network, 100 seeds) the Tracker does help, with 66% of seeds solved versus 52% at the default, but a fixed higher learning rate ($\eta = 0.1$) already solves 61%, so most of the gain is that of an effectively larger step rather than of online adaptivity. We also note that where a task is hard for representational rather than step-size reasons (sharp discontinuities, high-frequency targets), the default rate is already in the stable range and the init cap does not fire; the probe is, by design, silent there. These observations bound the claims to the one-shot init probe, on which the paper rests.

Table 11: Periodic in-training probing across regimes, at the default $\eta = 10^{-3}$. The Tracker's step-size growth helps only on a plateau-dominated toy, and there no more than a fixed higher learning rate would; on well-conditioned real tasks it degrades or diverges at every probe interval. Mean over seeds (5 for the real tasks, 100 for XOR); on the XOR toy the Tracker uses its best probe interval ($K = 20$), on the real tasks the default $K = 50$.

Regime (default $\eta = 10^{-3}$)	vanilla Adam	Watchdog	Tracker
Smooth: CIFAR-10 / ResNet-18 (test acc)	0.834	0.808	0.803
Smooth: AG News / Transformer (test acc)	0.902	0.904	DIV.
Plateau toy: 2-2 XOR (% solved)	52	52	66

In the same spirit we tested whether the probe could serve as an in-training *early-warning* signal for instability, rather than a controller. In our tests it did not provide a reliable early-warning signal for runtime divergence, for two reasons we observed across mini-batch (LSTM language modelling on War & Peace, CNNs) and full-batch Edge-of-Stability regimes: the reading does not discriminate (local curvature rises during *healthy* Edge-of-Stability training as much as before a blow-up), and the divergences we could induce were too abrupt to leave actionable lead time. On the evidence we have, the probe's value is therefore at initialisation (a curvature sensor and a safety cap), not as a runtime monitor; whether a refined variant could recover a usable signal we leave open.

Finally, the empirical scope of this paper is deliberately narrow. We report controlled experiments on three image-classification benchmarks (CIFAR-10 with a ResNet-18, Fashion-MNIST with a small two-conv CNN, and Imagenette with a standard ResNet-18 at 128px) and one text-classification benchmark (AG News with a small from-scratch Transformer); we do not test the rescue on large language models, on self-supervised vision pre-training, or at ImageNet scale. The empirical link between the line-search step and the top Hessian

eigenvalue is established for three architectures, not claimed universal. The Discussion below sketches the experiments that would, in our view, justify a stronger general claim.

6 Discussion

We have shown that classical Armijo line search, used as a probe rather than as the optimiser, robustifies Adam against a specific but common failure mode: an over-large initial learning rate. Its soundness rests on a clean, empirically reproducible link between the line-search step and the top Hessian eigenvalue.

In our framing, the probe is to Adam what airbags are to a car: a low-cost defence against a specific class of errors that does not change the normal driving experience. It leaves well-tuned training untouched and converts a reliably divergent run into a near-optimal one.

The mechanism is optimiser-agnostic in principle, and a first transfer check supports this: on CIFAR-10/ResNet-18, AdamW (Loshchilov & Hutter, 2019) diverges for every $\eta \geq 0.1$ exactly like Adam, and the direction-matched probe at the same fixed $\kappa = 2$ removes every divergence while holding test accuracy at 0.82–0.83 across the full grid (AdamW block of Table 3). Whether the same holds for optimisers with a different first-step geometry, such as RMSProp (Tieleman & Hinton, 2012), we leave open.

The main remaining direction is validation at larger scale: large language models, self-supervised pre-training, or ImageNet-scale training, where both the divergence boundary and the empirical link between the line-search step and the top Hessian eigenvalue may behave differently from the regime studied here. This is beyond our single-GPU budget and we leave it to future work, together with the question of whether the probe-as-controller idea is best combined with, rather than compared against, the parameter-free optimisers (D-Adaptation (Defazio & Mishchenko, 2023) and Mechanic (Cutkosky et al., 2023), which we discuss but do not run, would belong in that comparison).

7 Conclusion

A single Armijo backtracking line search (five forward evaluations and one backward pass) is a low-cost, Hessian-free sensor for local sharpness: the step inverts the *directional* curvature $q = g^\top Hg/\|g\|^2$ within the derived backtracking band, and $1/\alpha$ tracks λ_1 at Pearson -0.91 to -0.95 across three architectures: the textbook relation $\alpha^\star \approx 1/\lambda_1$, recovered for the price of a few forward passes rather than Lanczos iteration. The practical pay-off is a one-shot learning-rate cap that keeps Adam within a few points of its tuned accuracy across $\eta \in [10^{-3}, 3.0]$ on CIFAR-10, Fashion-MNIST, Imagenette and AG News, where vanilla Adam diverges from $\eta = 0.1$ on. Probing along Adam's own preconditioned direction makes the safety factor transferable: one fixed $\kappa = 2$ yields zero divergences on nine architectures and across the full grids of all four benchmarks, recovers full accuracy everywhere except the narrow-stable-range AG News Transformer, carries over to AdamW unchanged, and costs about one percent. We hope the low-cost curvature reading, more than the safeguard itself, encourages the use of line-search quantities as loss-landscape diagnostics.

References

Alexander Andreyev and Paolo Beneventano. Edge of Stochastic Stability: Revisiting the Edge of Stability for SGD. *arXiv preprint arXiv:2412.20553*, 2024. https://doi.org/10.48550/arXiv.2412.20553

Larry Armijo. Minimization of Functions Having Lipschitz Continuous First Partial Derivatives. *Pacific Journal of Mathematics*, 16(1):1–3, 1966. https://doi.org/10.2140/pjm.1966.16.1

Sanjeev Arora, Zhiyuan Li, and Abhishek Panigrahi. Understanding Gradient Descent on the Edge of Stability in Deep Learning. In *International Conference on Machine Learning (ICML)*, volume 162 of *Proceedings of Machine Learning Research*, pages 948–1024, 2022. https://proceedings.mlr.press/v162/arora22a.html

Jeremy M. Cohen, Simran Kaur, Yuanzhi Li, J. Zico Kolter, and Ameet Talwalkar. Gradient Descent on Neural Networks Typically Occurs at the Edge of Stability. In *International Conference on Learning Representations (ICLR)*, 2021. https://openreview.net/forum?id=jh-rTtvkGeM

Ashok Cutkosky, Aaron Defazio, and Harsh Mehta. Mechanic: A Learning Rate Tuner. In *Advances in Neural Information Processing Systems (NeurIPS)*, volume 36, pages 47828–47848, 2023. https://proceedings.neurips.cc/paper_files/paper/2023/hash/955499a8e2860ed746717c1374224c43-Abstract-Conference.html

Alex Damian, Eshaan Nichani, and Jason D. Lee. Self-Stabilization: The Implicit Bias of Gradient Descent at the Edge of Stability. In *International Conference on Learning Representations (ICLR)*, 2023. https://openreview.net/forum?id=nhKHA59gXz

Aaron Defazio and Konstantin Mishchenko. Learning-Rate-Free Learning by D-Adaptation. In *International Conference on Machine Learning (ICML)*, volume 202 of *Proceedings of Machine Learning Research*, pages 7449–7479, 2023. https://proceedings.mlr.press/v202/defazio23a.html

Aaron Defazio, Xingyu Alice Yang, Harsh Mehta, Konstantin Mishchenko, Ahmed Khaled, and Ashok Cutkosky. The Road Less Scheduled. In *Advances in Neural Information Processing Systems (NeurIPS)*, volume 37, pages 9974–10007, 2024. https://proceedings.neurips.cc/paper_files/paper/2024/hash/136b9a13861308c8948cd308ccd02658-Abstract-Conference.html

Timothy Dozat. Incorporating Nesterov Momentum into Adam. In *ICLR Workshop Track*, 2016. https://openreview.net/forum?id=OM0jvwB8jIp57ZJjtNEZ

Priya Goyal, Piotr Dollár, Ross Girshick, Pieter Noordhuis, Łukasz Wesolowski, Aapo Kyrola, Andrew Tulloch, Yangqing Jia, and Kaiming He. Accurate, Large Minibatch SGD: Training ImageNet in 1 Hour. *arXiv preprint arXiv:1706.02677*, 2017. https://doi.org/10.48550/arXiv.1706.02677

Jeremy Howard. Imagenette: A Smaller Subset of 10 Easily Classified Classes from ImageNet. https://github.com/fastai/imagenette, 2019.

Dayal Singh Kalra and Maissam Barkeshli. Why Warmup the Learning Rate? Underlying Mechanisms and Improvements. In *Advances in Neural Information Processing Systems (NeurIPS)*, 2024. https://doi.org/10.48550/arXiv.2406.09405

Dayal Singh Kalra, Jean-Christophe Gagnon-Audet, Andrey Gromov, Ishita Mediratta, Kelvin Niu, Alexander H. Miller, and Michael Shvartsman. A Scalable Measure of Loss Landscape Curvature for Analyzing the Training Dynamics of LLMs. *arXiv preprint arXiv:2601.16979*, 2026.

Diederik P. Kingma and Jimmy Ba. Adam: A Method for Stochastic Optimization. In *International Conference on Learning Representations (ICLR)*, 2015. https://doi.org/10.48550/arXiv.1412.6980

Aitor Lewkowycz, Yasaman Bahri, Ethan Dyer, Jascha Sohl-Dickstein, and Guy Gur-Ari. The Large Learning Rate Phase of Deep Learning: The Catapult Mechanism. *arXiv preprint arXiv:2003.02218*, 2020. https://doi.org/10.48550/arXiv.2003.02218

Nicolas Loizou, Sharan Vaswani, Issam H. Laradji, and Simon Lacoste-Julien. Stochastic Polyak Step-size for SGD: An Adaptive Learning Rate for Fast Convergence. In *International Conference on Artificial Intelligence and Statistics (AISTATS)*, volume 130 of *Proceedings of Machine Learning Research*, pages 1306–1314, 2021. https://proceedings.mlr.press/v130/loizou21a.html

Ilya Loshchilov and Frank Hutter. SGDR: Stochastic Gradient Descent with Warm Restarts. In *International Conference on Learning Representations (ICLR)*, 2017. https://openreview.net/forum?id=Skq89Scxx

Ilya Loshchilov and Frank Hutter. Decoupled Weight Decay Regularization. In *International Conference on Learning Representations (ICLR)*, 2019. https://openreview.net/forum?id=Bkg6RiCqY7

Konstantin Mishchenko and Aaron Defazio. Prodigy: An Expeditiously Adaptive Parameter-Free Learner. In *International Conference on Machine Learning (ICML)*, volume 235 of *Proceedings of Machine Learning Research*, pages 35779–35804, 2024. https://proceedings.mlr.press/v235/mishchenko24a.html

Maximus Mutschler and Andreas Zell. Parabolic Approximation Line Search for DNNs. In *Advances in Neural Information Processing Systems (NeurIPS)*, volume 33, pages 5405–5416, 2020. https://proceedings.neurips.cc/paper_files/paper/2020/hash/3a30be93eb45566a90f4e95ee72a089a-Abstract.html

Razvan Pascanu, Tomas Mikolov, and Yoshua Bengio. On the Difficulty of Training Recurrent Neural Networks. In *International Conference on Machine Learning (ICML)*, volume 28 of *Proceedings of Machine Learning Research*, pages 1310–1318, 2013. https://proceedings.mlr.press/v28/pascanu13.html

Sashank J. Reddi, Satyen Kale, and Sanjiv Kumar. On the Convergence of Adam and Beyond. In *International Conference on Learning Representations (ICLR)*, 2018. https://openreview.net/forum?id=ryQu7f-RZ

Vincent Roulet, Atish Agarwala, Jean-Bastien Grill, Grzegorz Swirszcz, Mathieu Blondel, and Fabian Pedregosa. Stepping on the Edge: Curvature Aware Learning Rate Tuners. In *Advances in Neural Information Processing Systems (NeurIPS)*, volume 37, pages 47708–47740, 2024. https://proceedings.neurips.cc/paper_files/paper/2024/hash/555479a201da27c97aaeed842d16ca49-Abstract-Conference.html

Leslie N. Smith. Cyclical Learning Rates for Training Neural Networks. In *IEEE Winter Conference on Applications of Computer Vision (WACV)*, pages 464–472, 2017. https://doi.org/10.1109/WACV.2017.58

Leslie N. Smith and Nicholay Topin. Super-Convergence: Very Fast Training of Neural Networks Using Large Learning Rates. In *Artificial Intelligence and Machine Learning for Multi-Domain Operations Applications (Proceedings of SPIE, volume 11006)*, article 1100612, 2019. https://doi.org/10.1117/12.2520589

Tijmen Tieleman and Geoffrey Hinton. Lecture 6.5—RMSProp: Divide the Gradient by a Running Average of Its Recent Magnitude. *Neural Networks for Machine Learning, Coursera*, 2012.

Sharan Vaswani, Aaron Mishkin, Issam H. Laradji, Mark Schmidt, Gauthier Gidel, and Simon Lacoste-Julien. Painless Stochastic Gradient: Interpolation, Line-Search, and Convergence Rates. In *Advances in Neural Information Processing Systems (NeurIPS)*, volume 32, pages 3727–3740, 2019. https://proceedings.neurips.cc/paper_files/paper/2019/hash/2557911c1bf75c2b643afb4ecbfc8ec2-Abstract.html

Zhewei Yao, Amir Gholami, Kurt Keutzer, and Michael W. Mahoney. PyHessian: Neural Networks Through the Lens of the Hessian. In *IEEE International Conference on Big Data*, pages 581–590, 2020. https://doi.org/10.1109/BigData50022.2020.9378171

A The negative result on the Golden-Section preselection

This project began as an attempt to build a bounded golden-section plus Armijo line-search optimiser (GGAO); the failure reported here motivated treating the line search as a measurement instead. The bounded golden-section line search on $[0, 1]$ consistently selects very small α ($\bar{\alpha} \approx 0.05$ throughout training) and drives the trajectory into regions of high λ_1 ($\bar{\lambda}_1 \approx 800$). Pure Armijo on the same architecture and initialisation

saturates at $\alpha = 1$ and stays in low-λ_1 regions ($\bar{\lambda}_1 \approx 200$). The α-λ_1 correlation, which is -0.91 ± 0.01 for pure Armijo on CIFAR-10/ResNet-18, drops to a non-significant -0.32 for GS+Armijo. The golden-section step finds spurious early local minima of the noisy mini-batch loss along the descent direction, where pure backtracking correctly accepts the largest step that satisfies sufficient decrease. We report this negative result here as a warning against bounded non-monotone line searches on stochastic deep-learning losses.

B Sensitivity to the safety factor κ

The rescue depends on a single scalar, the safety factor κ, which caps the user learning rate at $\kappa\,\bar{\alpha}_{\text{init}}$. To quantify how forgiving this choice is, we sweep $\kappa \in \{0.05, 0.1, 0.25, 0.5, 1.0\}$ for Adam-InitOnly on CIFAR-10/ResNet-18 at three representative learning rates (the optimal 10^{-3}, and two values at which vanilla Adam diverges), 3 seeds each. Table 12 reports the result.

Table 12: Sensitivity of Adam-InitOnly to the safety factor κ on CIFAR-10/ResNet-18 (10 epochs, mean±std over 3 seeds). "DIV." = all seeds diverged. Any $\kappa \leq 0.25$ keeps the rescue intact across the whole range; only $\kappa \geq 0.5$ lets divergence back in at large η. The recipe is thus insensitive to the exact value of κ within a broad band, so the one-minute calibration sweep need not be precise.

κ	$\eta = 10^{-3}$	$\eta = 10^{-1}$	$\eta = 1.0$
0.05	0.842 ± 0.007	$\mathbf{0.824 \pm 0.016}$	$\mathbf{0.829 \pm 0.019}$
0.1	0.813 ± 0.026	0.812 ± 0.012	0.813 ± 0.009
0.25	0.824 ± 0.012	0.794 ± 0.011	0.801 ± 0.020
0.5	0.836 ± 0.019	0.735 ± 0.033	0.725 ± 0.044
1.0	0.829 ± 0.021	DIV.	DIV.

At the optimal $\eta = 10^{-3}$ the cap rarely binds, so accuracy is near-constant across κ. At the misspecified rates the trend is monotone: smaller κ caps the learning rate more aggressively and preserves accuracy, whereas $\kappa = 1.0$ leaves the step essentially uncapped and Adam diverges exactly as in the vanilla baseline. The default $\kappa = 0.25$ used for CIFAR-10 sits comfortably inside the safe band; the rescue degrades gracefully rather than catastrophically as κ grows, which is why a coarse one-minute calibration suffices.

C Adam's divergence threshold and the safety factor κ

The architecture-independent choice of κ is made from the one-shot probe itself, through the safety sweep of Table 10 ($\kappa = 2$ for the direction-matched probe, zero divergences across nine architectures). As a complementary check we here locate the *absolute* divergence boundary of Adam and confirm it sits close to the line-search scale. For this single measurement we anchor to a low-variance estimate $\bar{\alpha}$ obtained by averaging the Armijo step over a short (200-step) warmup, rather than the raw init value, which is noisier and can saturate at $\alpha = 1$ on low-curvature initialisations; this gives $\bar{\alpha} = 0.0393$ on CIFAR-10/ResNet-18. We then trained Adam at $\eta = m \cdot \bar{\alpha}$ for $m \in \{0.25, 0.4, 0.5, 0.6, 0.7, 0.8, 0.9, 1.0, 1.5, 2.0, 5.0\}$. Table 13 summarises the result.

Table 13: Empirical determination of the absolute divergence boundary, expressed as a multiple of the warmup-averaged Armijo anchor $\bar{\alpha} = 0.0393$. Adam runs of one epoch (400 steps) on CIFAR-10/ResNet-18.

$m = \eta/\bar{\alpha}$	η	Outcome
$0.25, 0.4, 0.5$	$0.0099, 0.0160, 0.0200$	all stable
0.6	0.0240	diverged
0.7	0.0280	stable (boundary jitter)
$0.8, 0.9, 1.0, 1.5, 2.0, 5.0$	≥ 0.0319	all diverged

The boundary is sharp at $m \approx 0.5$–0.8. Choosing $\kappa = 0.25$ keeps Adam comfortably inside the stable region in all our experiments.

D Longer training schedule

The headline experiments use a deliberately short 10-epoch budget, where ResNet-18 reaches only 78–81% test accuracy, numbers that understate what the network normally attains. To check that the short schedule does not flatter (or undersell) the rescue, we re-ran the full learning-rate grid for 100 epochs with cosine annealing, 3 seeds (Table 14).

Table 14: Longer schedule on CIFAR-10/ResNet-18: 100 epochs with cosine annealing, mean±std over 3 seeds. "DIV." = all seeds diverged at the first update. At the realistic length the network reaches $\approx 93\%$; Adam-InitOnly retains that accuracy across the full 10^{-3}–3.0 range of initial learning rates, while vanilla Adam still diverges for any $\eta \geq 10^{-1}$.

η_{init}	10^{-3}	10^{-2}	10^{-1}	0.3	1.0	3.0
Vanilla Adam	0.935 ± 0.002	0.931 ± 0.001	DIV.	DIV.	DIV.	DIV.
Adam-InitOnly	0.935 ± 0.001	0.930 ± 0.004	0.926 ± 0.003	0.926 ± 0.001	0.927 ± 0.002	0.925 ± 0.002

At the optimal $\eta = 10^{-3}$ vanilla Adam and Adam-InitOnly are identical (0.935 both), confirming the probe is harmless when the learning rate is already well chosen. Across the entire range up to a 3000× misspecified $\eta = 3.0$ (where vanilla Adam diverges in the first step and has no entry to report for any $\eta \geq 10^{-1}$) Adam-InitOnly stays in $[0.925, 0.935]$, within one percentage point of the optimal configuration at every learning rate. The rescue is therefore not an artefact of the short 10-epoch budget: at a realistic training length the protected model reaches the same $\approx 93\%$ accuracy regardless of how badly the initial learning rate was chosen.

E Per-architecture results for the direction-matched probe

The aggregate rows of Table 9 average test accuracy over nine architectures with different chance levels and task difficulties, so the aggregate is meant only as a compact summary. Table 15 breaks it down per architecture at the discriminating 100×-too-large rate, for the recommended $\kappa = 2$; Figure 6 in the main text visualises this table. At this setting the direction-matched probe is the best variant on every architecture *and never diverges*, including the plain MLP, the lone partial failure at $\kappa = 3$ (Table 9), which is fully rescued here.

Table 15: Per-architecture test accuracy at the 100×-too-large learning rate ($\eta = 0.1$), mean over 3 seeds; a divergent run counts as 0, "DIV." = all seeds diverged. The Adam-direction probe uses the recommended $\kappa = 2$ (vanilla Adam and the grad probe as in Table 9); it diverges on none of the nine architectures.

Architecture	vanilla Adam	grad probe	Adam-dir probe ($\kappa = 2$)
ResNet-18 BN (CIFAR-10)	DIV.	0.57	**0.64**
VGG BN (CIFAR-10)	0.51	0.63	**0.68**
ResNet-18 GN (CIFAR-10)	DIV.	0.44	**0.53**
ResNet-18 no-norm (CIFAR-10)	DIV.	0.16 (2/3 d.)	**0.53**
CNN (Fashion-MNIST)	DIV.	DIV.	**0.90**
MLP (Fashion-MNIST)	DIV.	DIV.	**0.86**
LSTM (AG News)	0.29	0.33	**0.81**
Transformer no-warmup (AG News)	DIV.	0.25	**0.82**
Transformer wide (AG News)	DIV.	0.25	**0.84**

F Imagenette: a real-resolution control

This appendix gives the exact numbers behind the top-right panel of Figure 3. Imagenette (Howard, 2019) is the fastai ImageNet subset (10 classes, 9,469/3,925 train/val images); we train the standard, unmodified torchvision ResNet-18 (7×7 stride-2 stem with max-pooling) at 128×128 for 20 epochs (the small dataset yields only 37 steps per epoch), all other settings as in Section 4. At the well-tuned rate the probe changes nothing (0.767 vs 0.769).

Table 16: Imagenette at 128×128 with a standard ResNet-18 (20 epochs, mean±std over 5 seeds; best per column within each block in bold). "DIV." = all seeds diverged at the first update. The direction-matched probe uses the same fixed $\kappa = 2$ as everywhere else.

η_{init}	10^{-3}	10^{-2}	10^{-1}	0.3	1.0	3.0
Vanilla Adam	$\mathbf{0.769 \pm 0.021}$	$\mathbf{0.724 \pm 0.022}$	DIV.	DIV.	DIV.	DIV.
Direction-matched probe, fixed $\kappa = 2$ (no calibration)						
Adam-InitOnly (dir.)	$\mathbf{0.767 \pm 0.020}$	$\mathbf{0.750 \pm 0.011}$	$\mathbf{0.738 \pm 0.010}$	$\mathbf{0.742 \pm 0.017}$	$\mathbf{0.729 \pm 0.035}$	$\mathbf{0.718 \pm 0.040}$

G Experimental protocol

Every result is keyed by an integer seed that controls both data generation and model initialisation. Reported accuracies are means over the seed counts stated in each caption: five seeds for the CIFAR-10 sweep, three for the cross-architecture and correlation studies, four for the default-unsafe rescue, and up to one hundred for the XOR control. The wall-clock overhead figures come from a single interleaved, GPU-warmed benchmark rather than from runs collected across sessions, which we found to be contaminated by external load. The correlation study reports the line-search step against a PyHessian/Lanczos estimate of λ_1 computed on the same probe batch.